

We are IntechOpen, the world's leading publisher of Open Access books Built by scientists, for scientists

6,900

Open access books available

186,000

International authors and editors

200M

Downloads

Our authors are among the

154

Countries delivered to

TOP 1%

most cited scientists

12.2%

Contributors from top 500 universities



WEB OF SCIENCE™

Selection of our books indexed in the Book Citation Index
in Web of Science™ Core Collection (BKCI)

Interested in publishing with us?
Contact book.department@intechopen.com

Numbers displayed above are based on latest data collected.
For more information visit www.intechopen.com



Novel Enabling Technologies for Convergence of Optical and Wireless Access Networks

Janjun Yu¹, Gee-Kung Chang², Zhensheng Jia² and Lin Chen³

¹NEC Laboratories America

²Georgia Institute of Technology,

³Hunan University,

^{1,2}USA

³China

1. Introduction

New business models based on novel telecommunication technologies continue to dramatically change the way people live and work nowadays. People want to be always connected, with ultra-high speed data transfer, with high-quality video streaming and without face-to-face meeting. Thanks for the ~70 to 100% CAGR (cumulative annual growth rate) of mobile broadband growth, broadband mobile connectivity is now a necessity, which also leads to the increased capacity in the backbone and access networks. It is believed that wireless applications of HD-video are here and now and it is estimated that standard digital video will be unacceptable in future two years, HD-Video will be the new alternative to meet the increasing demand for broadband video services. Ultra uncompressed HD Video with (UHDV) 7680 x 4320 pixels (33 Mega pixels) plus 22.2 sound (24 channels in three layers) is expected to require larger than 40Gbps data speed. In addition to high-speed, symmetric and guaranteed bandwidth demands for future video services, next-generation access networks are driving the needs for the convergence of wired and wireless services to offer end users greater choice, convenience and variety in an efficient way. This scenario will require the delivery of voice, data and video services with mobility feature to serve the fixed and mobile users in a unified networking platform.

The most widely deployed access networks based on twisted-pair copper cable are approaching their upper limit of bandwidth-distance product (10 Mb/ s*km). For distance under 1.5 km, for example, asymmetric digital subscriber loop (ADSL) can deliver about 8 Mb/ s while the latest very-high-speed digital subscriber loop (VDSL) technology can deliver up to 26 Mb/ s for distances under 1 km. Another dominant access medium is the hybrid of fiber and coax cables (HFC). The guaranteed bandwidth per subscriber is only 2.8-5.6 Mb/ s for the downstream and 0.15-0.3 Mb/ s for the upstream due to the bandwidth shared within a cell (500-1000 subscribers). It is quite obvious that the two technologies cannot meet the bandwidth demands for the future video services and will have limited lifetimes. With the trend to deploy optical fiber deeper and deeper and the development of

Source: Frontiers in Guided Wave Optics and Optoelectronics, Book edited by: Bishnu Pal,
ISBN 978-953-7619-82-4, pp. 674, February 2010, INTECH, Croatia, downloaded from SCIYO.COM

highly recognized passive optical network (PON), it is expected that time-division multiplexing PON (TDM-PON) and wavelength-division multiplexing PON (WDM PON) will be the most promising candidates for next-generation access systems. A TDM PON, including asynchronous-transfer-mode (ATM) and broadband PON (A/ BPON), Ethernet PON (EPON) and Gigabit PON (GPON), shares a single transmission channel to be a satisfactory solution for the near future bandwidth needs. A WDM PON provides point-to-point optical connectivity to multiple end users through a single feeder fiber and will be a future-proof access network. On the other hand, broadband wireless access (BWA) technologies have surged in popularity because they are more convenient, scalable and flexible for roaming connections. Most widely used technologies are local multipoint distribution service (LMDS) and multi-channel multipoint distribution service (MMDS). World Interoperability for Microwave Access (WiMAX) is another BWA technology being standardized by IEEE 802.16. These technologies can provide wireless connection but severely constrained by the required bandwidth especially for the video-centric services with high-definition TV (HDTV) quality.

To make full use of huge bandwidth offered by fiber and mobile feature presented via wireless scheme, the integration of wireless and optical networks is a potential solution for increasing capacity and mobility as well as decreasing costs in the access network. Thus, radio-over-fiber (ROF) based optical-wireless networks came into play and has emerged as an affordable alternative solution in environments such as conference center, airport, hotels, shopping malls – and ultimately to homes and small offices. The integration of optical and wireless means the convergence of two conventional technology field - radio frequency (RF) for wireless access and optical fiber for wired transmission. Long-range links are provided by optical fiber and the last tens of meters are accomplished by wireless. The requirement of more wireless bandwidth leads to spectral congestion at lower microwave frequencies in current wireless access networks. Millimeter-wave systems have the unique potential to resolve the scarcity of access bandwidth and the spectral congestion. In this situation, it is necessary to minimize the cost of the base station (BS) and shift the system complexity and expensive devices to the central office (CO) because the BS picocell has small coverage due to high atmospheric attenuation in the mm-wave band. Fig. 1 depicts the generic architecture of optical-wireless network and the enabling technologies we will discuss in the paper. At the central office (CO), the optical mm-wave signals are generated and mixed by using cost-efficient all-optical approaches. Optical networking technologies are leveraged to reach the longer transmission distance over single mode fiber (SMF) and integrate with WDM PON between the BS and CO. The BS design goal is to make the full-duplex operation and dual-service provision possible with a simple and low-cost way, which typically involves the choice of optical up-conversion technologies for overall architecture planning. In this book chapter, we will demonstrate several key techniques for next-generation hybrid optical-wireless networks. Optical mm-wave signal generation and up-conversion with low-cost approaches are vital to future real deployment in access networks. Different schemes for optical mm-wave generation, up-conversion and transmission are compared. For all-optical up-conversion technique, the techniques based on external modulation (OCS and phase modulation) are the promising solution for downlink transmission in terms of required input power, transmission performance against dispersion in the fiber, support for WDM PON, mixing bandwidth, stability and system configuration. Using orthogonal

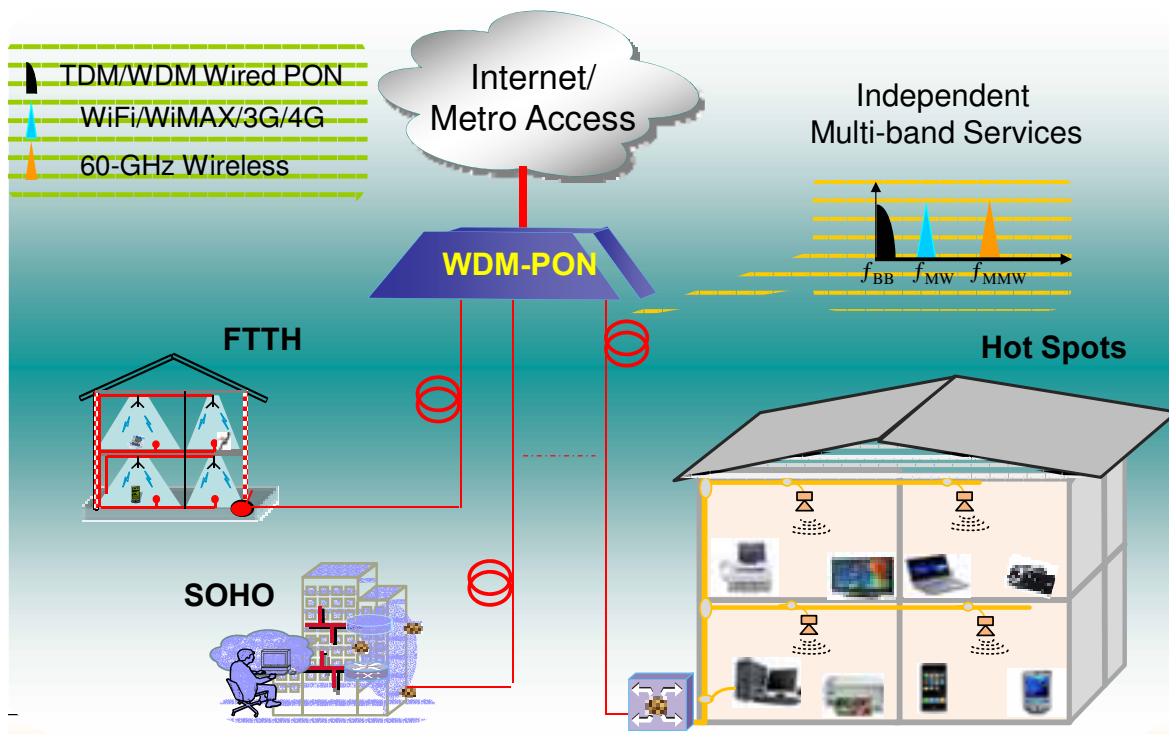


Fig. 1. A generic architecture of an optical-wireless network.

frequency division multiplexing (OFDM) modulation format, the spectral efficiency can be significantly increased and the fiber dispersion can be further mitigated. We will also demonstrate the possibility to seamlessly integrate RoF with WDM-PON networks for simultaneously serving multiple end users by leveraging the existing PON networks.

In the case of uplink, the network architecture consisting of a single light source at the CO and the reuse of the downstream wavelength at the base station BS is an attractive solution for consolidated bidirectional connection as it requires no additional light source and wavelength management at the BS. Several schemes for realizing full-duplex transmission are described in this chapter based on wavelength reuse to avoid the need of the light source at the BS. The delivery of 16Gb/s super broadband OFDM optical signals are also introduced in the transmission of 50m grade-index fiber.

To exploit the benefits of both wired and wireless technologies, carriers and service providers are actively seeking a convergent network architecture to deliver multiple services to serve both fixed and mobile users. This can be accomplished by using hybrid optical-wireless networks, which not only can transmit wireless signals at the BS over fiber, but also simultaneously provide the wired and wireless services to the end users. A super-broadband access testbed is presented to deliver both wired and wireless services simultaneously via an optical fiber or air, and an order of magnitude larger access bandwidth than the state-of-the-art Wi-Fi systems can be provided. A campus-wide field trial is demonstrated for RoF system to transmit uncompressed 270-Mbps standard definition (SD) and 1.485-Gbps high definition (HD) real-time video contents carried by 2.4-GHz radio and 60-GHz millimeter wave signals, respectively, between two on-campus research buildings distanced over 2.5-km standard single mode fiber (SMF-28) through the Georgia Institute of Technology's (GT) fiber network.

2. Optical mm-wave up-conversion for downstream

An intermediate frequency (IF) or baseband signal can be transmitted over optical fiber to the BS, where the baseband or IF signal are up-converted to mm-wave carriers for broadcasting in the air. In this way, the signal transmission over optical fiber is less severely affected by chromatic dispersion. However, this approach requires frequency up-conversion at the BS with a mm-wave mixer and a local oscillator (LO) signal. Generating mm-wave frequencies using electrical devices is challenging because of the bottleneck of high-speed electronic processing. Additionally, because of the requirement of numerous BSs in optical mm-wave access networks, this approach significantly increases the cost and complexity of the BS. The most promising solution is to use optical approaches for mm-wave signal generation at the CO. Over the past few years, many groups have conducted research to develop optical mm-wave generation, up-conversion and transmission techniques. Traditionally, three different methods exist for the generation of mm-wave signals over optical links with intensity modulation: direct modulation, external modulation and remote heterodyning. Direct modulation is by far the simplest, and 40GHz mm-wave signal is generated by using this modulation technique. However, due to the limited modulation bandwidth of the laser, there is no 60GHz mm-wave signal generation by using direct modulation. The configuration of external modulation is simple and can be used to generate optical mm-wave, but it has some disadvantages that limit its implementation at mm-wave because high cost for driving signals and low dispersion tolerance. The double-sideband (DSB) carrier modulation format severely suffers the chromatic dispersion when the signals

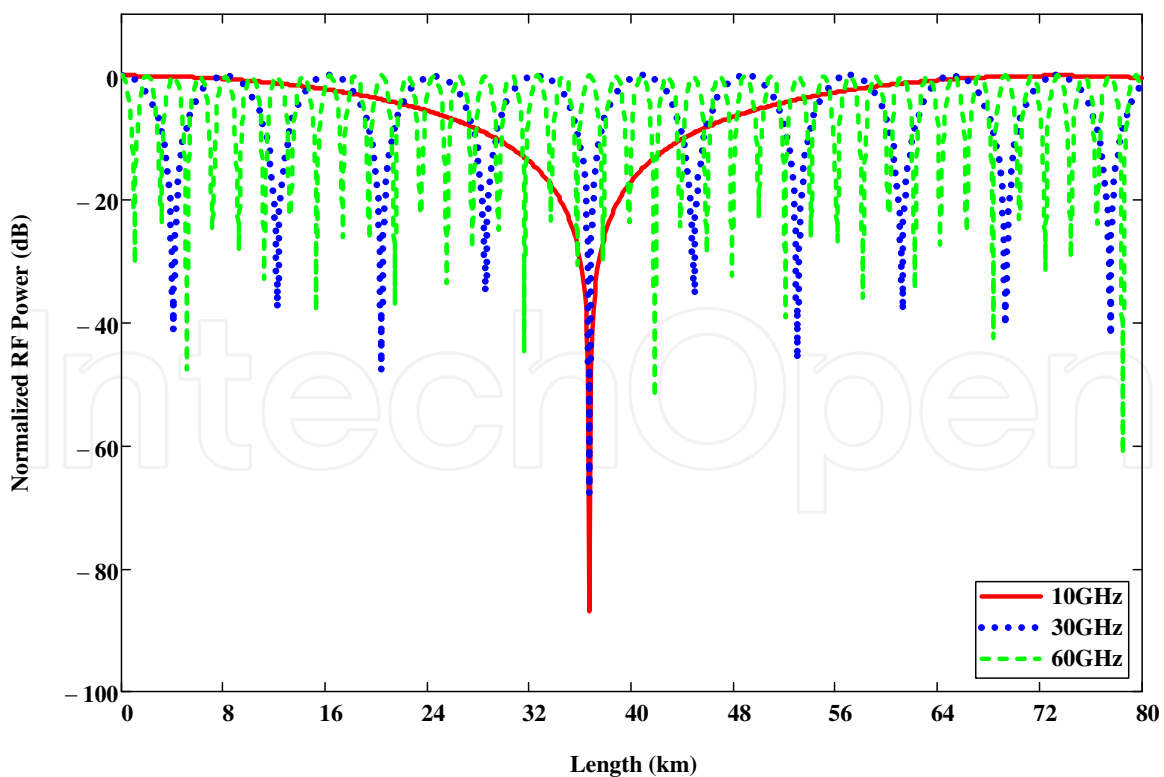


Fig. 2. Normalized received RF power for optical DSB modulation as a function of transmission distance in dispersive optical fiber ($D: 17\text{ps}/\text{km}/\text{nm}$, wavelength: $1.55\mu\text{m}$)

propagate along a dispersive fiber because two sidebands experience different amount of phase shift compared to original carrier. The received RF power of the mm-wave signal varies depending on the relative phase difference between two beating components, as shown in Fig.2. It can be seen that the RF power varies in a periodic manner along the fiber. For optical heterodyning technique, two or more optical signals are simultaneously transmitted and are heterodyned in the receiver. However, it requires either a precisely biased electro-optic modulator or a complex laser to reduce the severe phase noise, which greatly adds to the cost and complexity of the system.

Recently, several new approaches for up-conversion of radio signals have been reported. These techniques, based on nonlinear effects in wave-guide device, exhibit low conversion efficiency and need very high input optical power. The scheme based on cross-gain modulation (XGM) in semiconductor optical amplifier (SOA) requires a large input power to saturate the gain of SOA. The scheme by using cross-phase modulation (XPM) in SOA Mach-Zehnder Interferometer (SOA-MZI) loosens the requirement for the input power, however, the complicated conversion structure and nonlinear crosstalk among multiple channels are major hurdle to greatly limit the signal quantity of wireless end users. Here some all-optical up-conversion schemes in direct modulation laser, highly-nonlinear dispersion-shifted fiber (HNL-DSF), electroabsorption modulator (EAM), external intensity, integrated modulator and phase modulator will be introduced.

2.1 Optical mm-wave generation by a DML

Fig. 3 shows the principle to generate optical mm-wave signals by using only one DML and wavelength reuse for uplink connection. In the central office, a wideband DML is used to generate optical mm-wave signal. The RF signals are generated by an electrical mixer which mixes the LO and downstream data. In the base station an optical interleaver with two

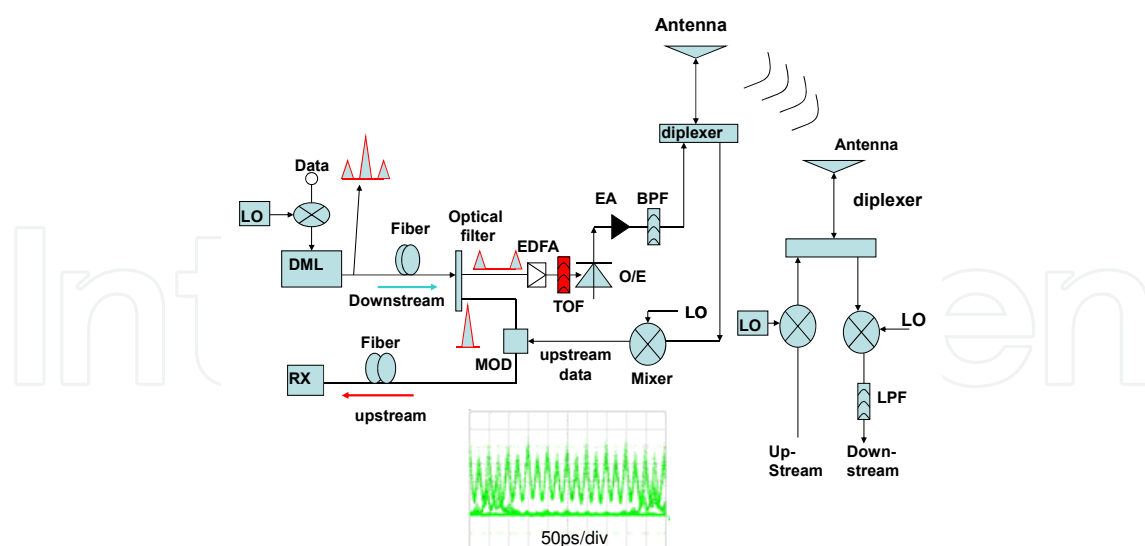


Fig. 3. Mm-wave signal generation by using one DML and ROF network configuration with both down and upstream connection and source-free in the base station. DML: direct-modulation laser, O/ E: optical/ electrical converter, RX: receiver, EA: electrical amplifier, LFP: low-pass filter, BPF: band-pass filter, MOD: modulator. The eye diagram (50ps/ div) of optical mm-wave signal at 40GHz generated from the DML after one 25GHz optical interleaver is inserted.

output ports or cascaded an optical circulator and a fiber Bragg grating (FBG) is used to separate the optical carrier and the first-order sidebands. After the optical interleaver, the two peaks of the first-order sidebands will be beat to generate mm-wave signals with a double repetitive frequency of the RF signal when they are detected by a downlink receiver. The bandwidth of the commercial DML can be over 20GHz, so the repetitive frequency of the optical mm-wave can go up to 40GHz. The separated optical carrier can be used to carry the uplink optical signals. The base-band uplink data is used to drive an external modulator to generate optical uplink optical signals before it is transmitted over the fiber to the central office. In one experiment, one commercial DML with central wavelength of 1550nm biased at 57mA was used to generate lightwave. The output power biased at 57mA of the DML is 4dBm, and 3dB bandwidth of the DML is larger than 20GHz. The RF signals are generated by using an electrical mixer to combine the 20GHz RF clock (sinusoidal wave) and 2.5Gb/s electrical baseband signal (downstream data). Then the mixed RF signals are boosted to 2.7Vp-p to drive the DML. The repetition frequency of the optical mm-wave is 40 GHz as shown in the inserted figure in Fig. 2.

2.2 FWM in HNL-DSF

Four-wave mixing (FWM) is one of the important nonlinear effects to generate new waves or parametric amplification, especially for effectively ultra-fast response by using HNL-DSF. Relying on the third-order electric susceptibility and beating process with the frequency phase-matching condition when light of three or more different wavelengths is launched into HNL-DSF, it is possible to realize terahertz all-optical mixing or up-conversion as shown in Fig.4. Two pumping waves $\omega_{OCS} - \omega_{RF}$ and $\omega_{OCS} + \omega_{RF}$ are generated by using optical carrier suppression (OCS) technologies, where ω_{RF} is the RF sinusoidal clock frequency. The converted signal ω_{con} may then be determined by

$$\omega_{con} = (\omega_{OCS} - \omega_{RF}) + (\omega_{OCS} + \omega_{RF}) - \omega_s = 2\omega_{OCS} - \omega_s \quad (1)$$

where ω_s is the input signal light. The two pumping waves are set to coincide with the fiber zero-dispersion wavelength to generate beating grating in HNL-DSF efficiently, which will modulate the input signal ω_s to produce two sideband waves with the frequency shift

$$\omega_{con} \pm |(\omega_{OCS} - \omega_{RF}) - (\omega_{OCS} + \omega_{RF})| = \omega_{con} \pm 2\omega_{RF} \quad (2)$$

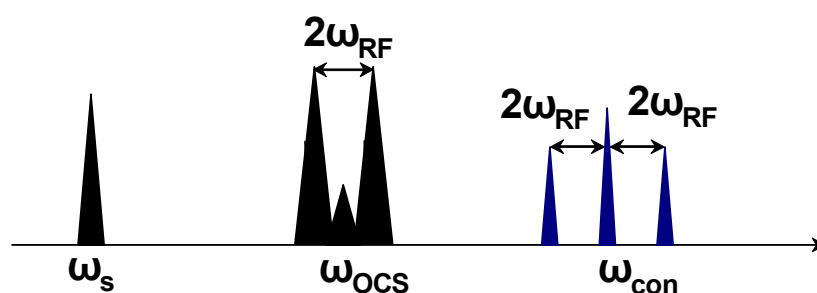


Fig. 4. Schematic of FWM based all-optical up-conversion.

The power is determined by the third-order nonlinearity susceptibility $\chi^{(3)}$ and the fiber parameters. Since FWM is independent of the signal bit rate and coding format, which can

be used to realize simultaneous up-conversion of multiple WDM signals and easily integrated with passive optical access networks. In addition, the HNL-DSF has high Raman gain to assist the FWM process in terms of conversion efficiency and bandwidth. Table 1 shows transmission characteristics of the HNL-DSF used in these experiments. The fiber was made by OFS Denmark and has a nonlinear coefficient γ of $10 \text{ W}^{-1}\text{km}^{-1}$ with the length of 1 km.

Using this scheme, eight WDM signals with the channel spacing of 3.2 nm are generated from eight DFB lasers and modulated by a LiNbO_3 Mach-Zehnder (M-Z) modulator driven by 2.5-Gb/s baseband signals. The modulated WDM signals are then transmitted over 10-km SMF to de-correlate the signals before the up-conversion. OCS modulation scheme is used to generate a 40-GHz optical local-oscillator (LO) signal as the two FWM pumping signals. It is realized by driving a dual-arm M-Z modulator biased at V_π with two complementary 20-GHz radio frequency (RF) sinusoid waveforms. To increase the FWM conversion efficiency and broaden the conversion bandwidth, a backward Raman pump is utilized. The advantages for FWM based all-optical up-conversion is that FWM is transparent to the signal bit-rate and modulation formats, which is easy to realize up-conversion for different WDM signals. In addition, due to the ultra-fast nonlinear response of the fiber, it is possible to realize THz waveform all-optical mixing or up-conversion. Meanwhile, the HNL-DSF has higher Raman gain compared to standard DSF, which can be utilized to assist the FWM process.

Characteristics	Measured value
Attenuation coefficient	0.4 dB/ km
Zero-dispersion wavelength	1561.0 nm
Dispersion slope (at zero-dispersion wavelength)	0.03 ps/ nm^2 / km
Nonlinear coefficient	$10 \text{ W}^{-1}\text{km}^{-1}$
Length	1 km
Raman Gain	4 - 8.5 dB

Table 1. Transmission characteristics of HNL-DSF.

To overcome polarization sensitivity when one single pump is employed, a novel scheme with dual-pumps is proposed and experimentally demonstrated. OCS can be realized when an intensity modulator (IM) is biased at null point, as shown in Fig. 1(b). If we assume that the modulator is driven by a RF sinusoidal wave signal with a repetitive frequency of f . After the IM, two subcarriers with wavelength spacing of $2f$ will be generated from a CW lightwave by carrier suppression scheme. The generated two lightwaves have the same polarization direction, optical power, and locked phase. The frequency spacing is exactly controlled by the RF frequency of the sinusoidal wave on the modulator. In our previous investigation, we have shown that the polarization-insensitive wavelength conversion can be realized when two pump lightwaves have the same polarization direction, and the converted signal locates the same side with the original signal. Another condition to meet the polarization-insensitive wavelength conversion is that the original signal should be far away from the pumps. This condition can be easily realized in the real system. The proposed scheme to realize all-optical up-conversion is shown in Fig. 5. To simplify the system, we only consider single channel input baseband signal. In our previous experiment,

two pumps are generated from different laser source; therefore, their phase is not locked. Moreover, in order to maintain the same polarization direction, we need to use polarization controller (PC) or polarization maintaining fiber (PMF) to keep the two lightwaves have the same polarization direction. If the emitting wavelength of the laser is not stable, the wavelength of the converted signal will be drifted. Obviously, if we use OCS scheme to generate two pump lightwaves, these problems, like polarization direction and frequency spacing, can be effectively solved. As shown in Fig. 5(a), the single channel baseband signal with the dual-pumps generated by OCS are injected into the nonlinear medium such as nonlinear fiber or semiconductor optical amplifier. Due to FWM in the nonlinear medium, new optical components will be generated. To simplify this figure, we only consider the first-order FWM, and the high-order FWM is neglected. Also, we do not consider the FWM between the pumps. We can see that two converted signals are generated as shown in Fig. 5(b). The two converted signals have the same polarization direction, and their phase is locked. In this scheme, the optical signals similar to a double sideband (DSB) are generated which includes two converted signals and original signal after wavelength conversion. Then we use optical filter, an optical interleaver is optimal, to remove the original signal as shown in Fig. 5(c). In this way, the two converted new signals with channel spacing of $4f$ can be obtained after FWM process in the nonlinear medium. By using this scheme, 60GHz optical mm-wave signal, which carries 7.5Gb/s baseband signal, is generated, and one eye diagram is shown in Fig. 5(d).

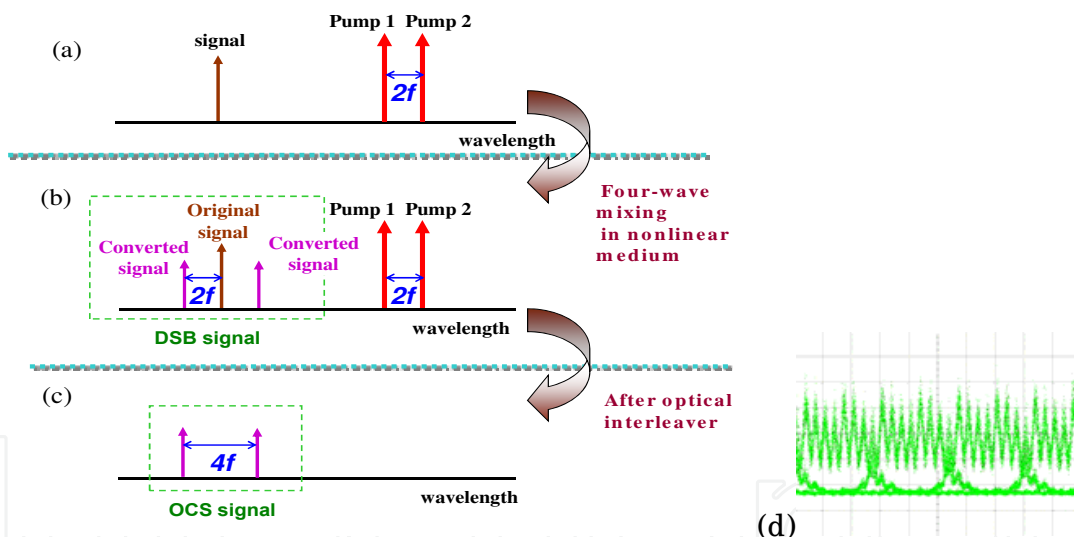


Fig. 5. All-optical up-conversion based on polarization-insensitive FWM in nonlinear medium. (d) Eye diagram of 10Gb/s signal carried by 60GHz mm-wave (50ps/div).

2.3 XPM in HNL-DSF

Cross-phase modulation (XPM) in the nonlinear optical loop mirror (NOLM) and straight pass in HNL-DSF is also possible to realize all-optical up-conversion for more wavelength channels without any interference and saturation effect limitation. A conceptual diagram by using OCS as the control signal is shown in Fig. 6(a) and (b). Regarding the NOLM architecture, the symmetry between the counter-propagation paths of the probe signal is broken due to XPM induced phase shift by the control signal. So the NOLM is changed into the mixer between the probe and control signal. For the straight-line structure, while

propagating in the HNL-DSF, the intensity of the control signal modulates the electric field of the probe data signal via XPM effect. Therefore, the RF sinusoidal clock is imposed onto the probe signal as the sidebands. Since the NOLM suffers from the stability problems due to the sensitive polarization state in the loop, XPM-based up-conversion in straight-line HNL-DSF are simpler and more robust. By using this nonlinear effect with a straight-line architecture, 16 channels at 2.5Gb/s are upconverted to 40GHz carrier in recent experiment. It is noted that the optical carrier-to-sideband ratio (CSR) has influences on the system performance because the mm-wave signals are generated by the interplay between the optical powers in the carrier and sideband or the two sidebands themselves. CSR refers to carrier-to-sideband ratio, the ratio of the optical power in the optical carrier to that of the first-order sideband within a defined resolution bandwidth (here set as 0.01nm). While maintaining the CSR at 13 dB, the measured receiver. This scheme exhibits very good conversion performance at high data rate and can provide more wavelength channels by being extended into the whole optical fiber transmission band without any interference and saturation effect limitation.

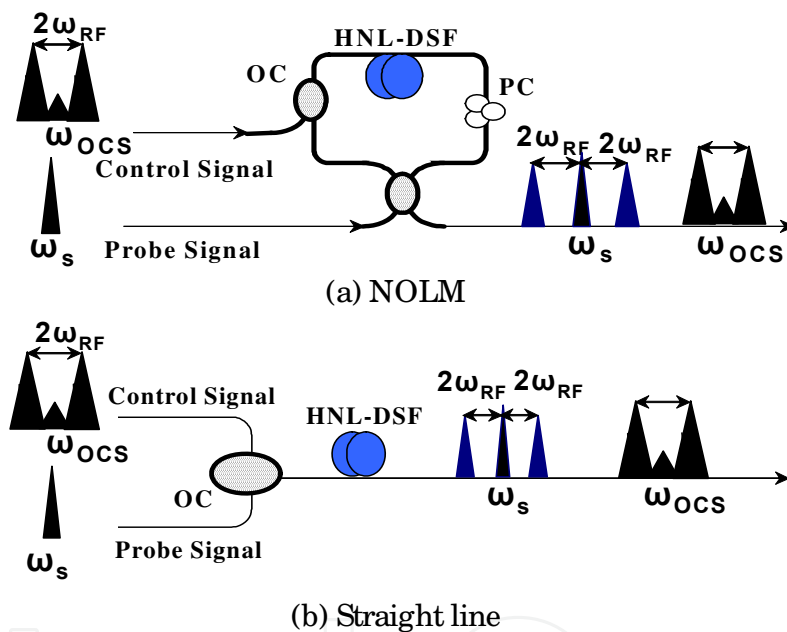


Fig. 6. Concept of using XPM-based all-optical up-conversion.

2.4 XAM in EAM

The principle of up-conversion based on EAM is similar to its wavelength conversion mechanism at high bit rate, the main difference from wavelength conversion is that the modulated data signal will be used to replace the CW source. The experimental setup is shown in Fig. 7.

An EAM (CyOptics: EAM 40) with 3-dB bandwidth of 32 GHz, fiber-to-fiber insertion loss of 8 dB and polarization sensitivity lower than 1 dB is used to realize the signal up-conversion. Optical LO signals are generated by using OCS modulation scheme with larger than 25 dB of the carrier suppression ratio. The electrical signal and waveform is also inserted as an inset in Fig. 7. This scheme has some advantages such as low power consumption, compact size, polarization insensitivity, easy integration with other devices and higher speed operation due to EAM inherent characteristics.

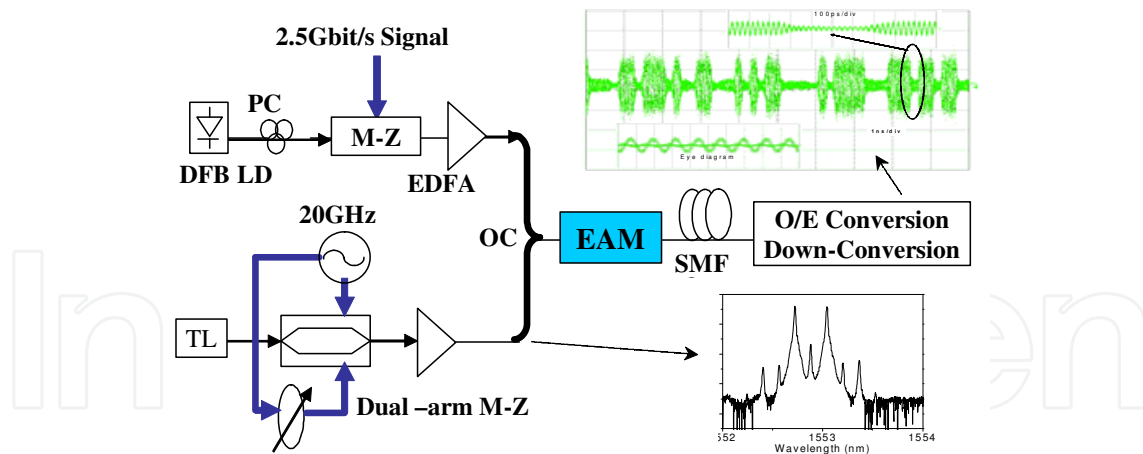


Fig. 7. Experimental setup of XAM-based all-optical mixer in EAM.

2.5 External intensity modulation

External modulation is another choice to up-convert mm-wave signals for ROF systems. Essentially, three different schemes exist for the generation and transmission of mm-wave signals over optical links with intensity modulation: double-sideband (DSB), single-sideband (SSB) and OCS modulation scheme. Fig. 8 shows optical mm-wave generation based on DSB, SSB and OCS modulation schemes respectively, and the corresponding optical spectra and eye diagrams after mixing with the 40-GHz RF signal are also inserted. Baseband data signal is generated by an M-Z modulator driven by 2.5-Gb/s PRBS electrical signal with a word length of $2^{31}-1$. For DSB modulation scheme, the M-Z modulator 2 is biased at $0.5 V_{\pi}$ and the frequency of the driven RF signal is 40 GHz. The generated mm-

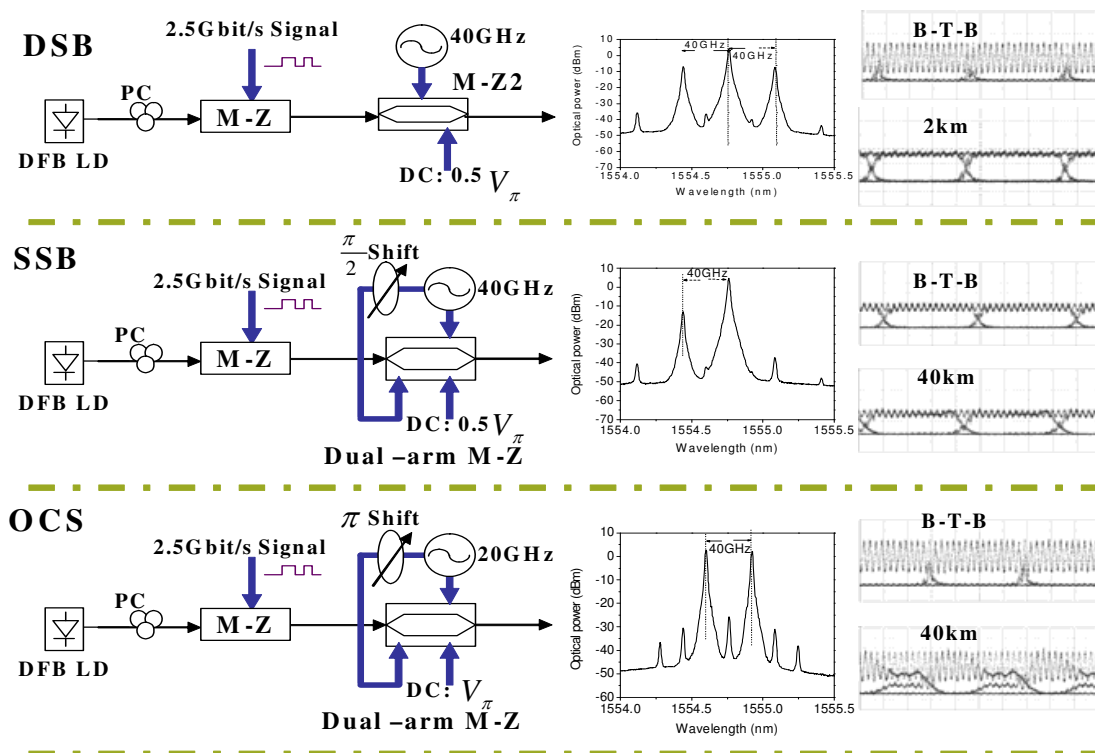


Fig. 8. Up-conversions using DSB, SSB and OCS techniques.

wave will occupy over 80-GHz bandwidth because it has two sidebands. Since the two sidebands have different velocities in SMF, the RF power at 40 GHz will disappear after transmitting over a certain length of SMF. As an example, the eye diagram after transmission over 2 km is inserted in Fig.8. It is seen that RF power at 40 GHz is almost faded, which leads to a large power penalty. The measured BER curves in Fig.9 show the power penalty is 17 dB at a BER of 10^{-10} after 2km transmission. These results indicate that DSB modulation based scheme is not suitable to a large area access network. A dual-arm M-Z modulator is employed to achieve SSB modulation. The two electrical RF signals to drive the dual-arm M-Z modulator has a phase shift of $\pi/2$, and the DC bias is at $0.5V_{\pi}$. The generated optical mm-wave will only occupy 40-GHz bandwidth, but the optical CSR is generally larger than 15 dB, which means it is full of DC components at the peak of center wavelength; hence it results in low receiver sensitivity. Fig. 9 shows the receiver sensitivity of back-to-back for SSB modulation is around 10 dB lower than that of DSB modulation. Although there is no power penalty after 20-km transmission, it is more than 5 dB after 40-km transmission due to fiber dispersion and large CSR. When the phase of the two electrical RF signals to drive the dual arm M-Z modulator is set to π difference and the DC bias is at the minimal intensity-output point or V_{π} , OCS modulation is realized. In this scheme, only 20-GHz RF signal is needed and the bandwidth for the M-Z modulator is also only 20 GHz, moreover the generated optical spectrum just occupies 40-GHz bandwidth. At BER of 10^{-10} , the receiver sensitivity of B-T-B mm-wave signal is -39.7 dBm, which is similar to that of the millimeter signal generation based on DSB modulation. There is no power penalty after transmission over 20 km, and the power penalty is less than 2 dB after 40-km transmission. The electrical eye diagrams after 10-km and 50-km transmission are shown as an inset (i) and (ii) in Fig. 9. These results show the mm-wave generated by OCS modulation can be used in large area access networks.

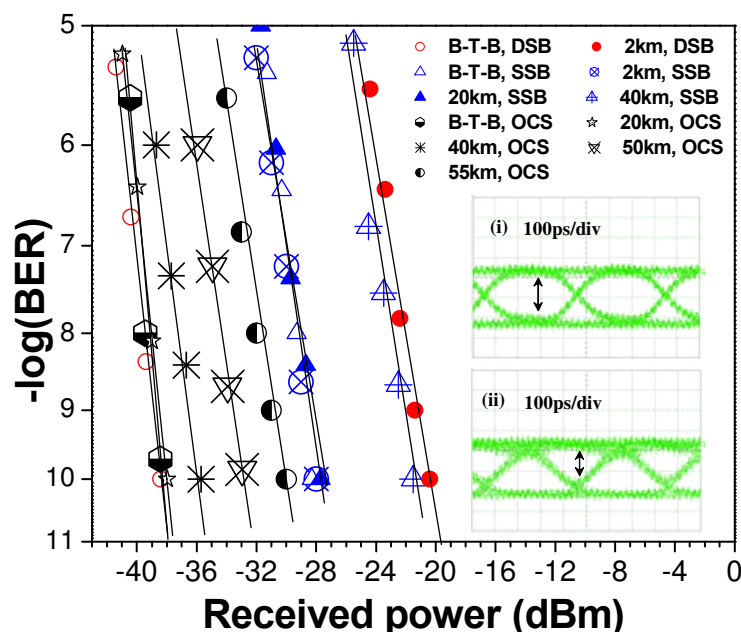


Fig. 9. BER curves with different mm-wave generation schemes.

Since the optical mm-wave has two peaks after OCS modulation, it will suffer from dispersion in fiber when transmission over SMF. The pulse width of the 2.5-Gb/s signal

carried by the optical mm-wave is approximately 400 ps. The two peaks with a wavelength spacing of 0.32 nm will have a walk-off time of 400 ps caused by fiber dispersion after transmission over 74-km SMF with a group velocity dispersion (GVD) of 17 ps/ nm/ km, which means the eye will be fully closed after this distance. While considering the limited rise and fall times of the optical receiver and electrical amplifier, the maximum delivery distance will be shorter. Fig. 10 clearly shows the evolution of optical eye diagrams at different transmission distance. The un-flat amplitudes of the optical carriers at 40 GHz as shown in Fig. 10 (b) are caused by chromatic dispersion. Previous investigations show that fiber dispersion causes the amplitude fluctuation of the carrier but the RF power at 40 GHz does not disappear when the carrier is a pure dual-mode lightwave. Fig. 10 (d) shows that the eye is almost closed after the optical mm-wave is transmitted over 60 km.

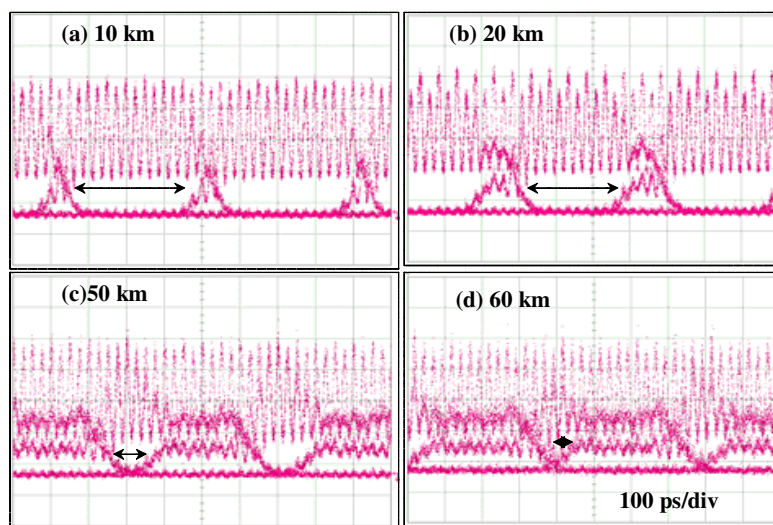


Fig. 10. Optical eye diagrams at different transmission distance.

By using the OCS modulation scheme, 32x2.5-Gb/ s DWDM signals after transmission over 40 km are simultaneously up-converted to integrate with WDM PON networks. In this experiment, 32 DFB laser array is used to realize 32 wavelength signals from 1536.1 nm to 1560.9 nm with adjacent 100 GHz spacing. An AWG is used to combine the 32 CW lightwaves before modulation by an M-Z. The generated 32x2.5-Gb/ s signals are transmitted over 40 km for simulation the metro optical network before they are up-converted by using a dual-arm M-Z based on OCS technique. The up-converted mm-waves are amplified by an EDFA to get a power of 20 dBm before transmission over variable length SMF. At the receiver, the desired channel is selected by using the identical O/ E and down-conversion components as in forenamed setup. The measured power penalty is smaller than 2dB for all channels after transmission over 40km.

The up-conversion signals based on OCS modulation scheme have shown the best performance such as the highest receiver sensitivity, the highest spectral efficiency, and the smallest power penalty over long distance delivery compared to DSB and SSB modulation scheme.

There are some modified schemes to realize all-optical up-conversion based on external intensity modulator. One scheme is to use low RF frequency to drive an intensity modulator to generate optical mm-wave signal with frequency quadrupling technique. The principle is shown in Fig. 11. A LiNbO₃ intensity modulator (IM) is employed to generate optical mm-

wave with low-frequency RF. Downstream data and RF signal at quarter of LO frequency are mixed by using subcarrier multiplexing (SCM) technique then to drive the IM. To realize an optical mm-wave carrier with four times of LO frequency, the modulator needs to be de-biased at the peak output power when the LO signal is removed. If the repetitive frequency of the RF microwave source is f_0 , the frequency spacing between the second-order modes is equal to $4f_0$ while the first-order modes are suppressed. As an example, the output optical spectrum shown in Fig. 11 is for the case of a 10 GHz modulation frequency. From the figure, it can be seen that the frequency spacing of the second-order modes is 40 GHz and the first-order sidebands are also suppressed. Taking the advantage of this property can dramatically lower the bandwidth requirements for the optical modulator and allows the use of a much lower frequency electrical drive signal. This can greatly reduce the cost of the system and makes it more practical to use.

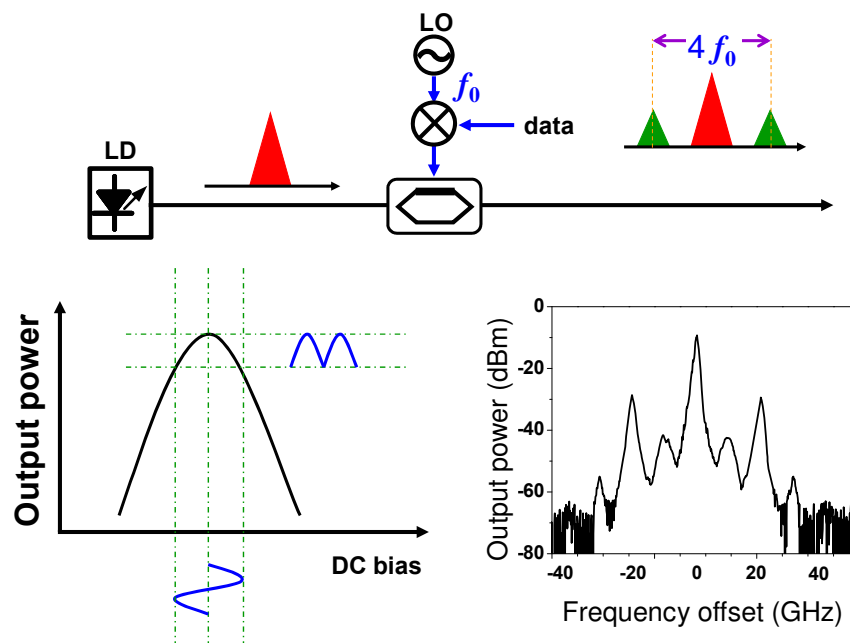


Fig. 11. Principle of frequency quadrupling scheme. Resolution of the optical spectrum is 0.01 nm.

Fig. 12 shows another scheme to generate optical mm-wave without optical filtering by using an integrated modulator. A conceptual diagram of optical carrier suppressed millimeter-wave signal generation using a frequency quadrupling technique without any optical filter. An external integrated MZM that consists of three sub-MZMs is key to generating optical millimeter-wave signals. One sub-MZM (MZ-a or MZ-b) is embedded in each arm of the main modulator (MZ-c). The optical field at the input of the integrated MZM is defined as (1) where is the amplitude of the optical field and is the angular frequency of the optical carrier. MZ-a and MZ-b are both biased at the full point. Electrical driving modulation signals sent into MZ-a and MZ-b are and , respectively. The odd sidebands are suppressed after passing through MZ-a and MZ-b. Since the MZ-c is biased at the null point, the optical carrier is suppressed when the lightwave passes through this integrated modulator, and only the second sidebands are left, hence a quadrupling mm-wave signal is generated.

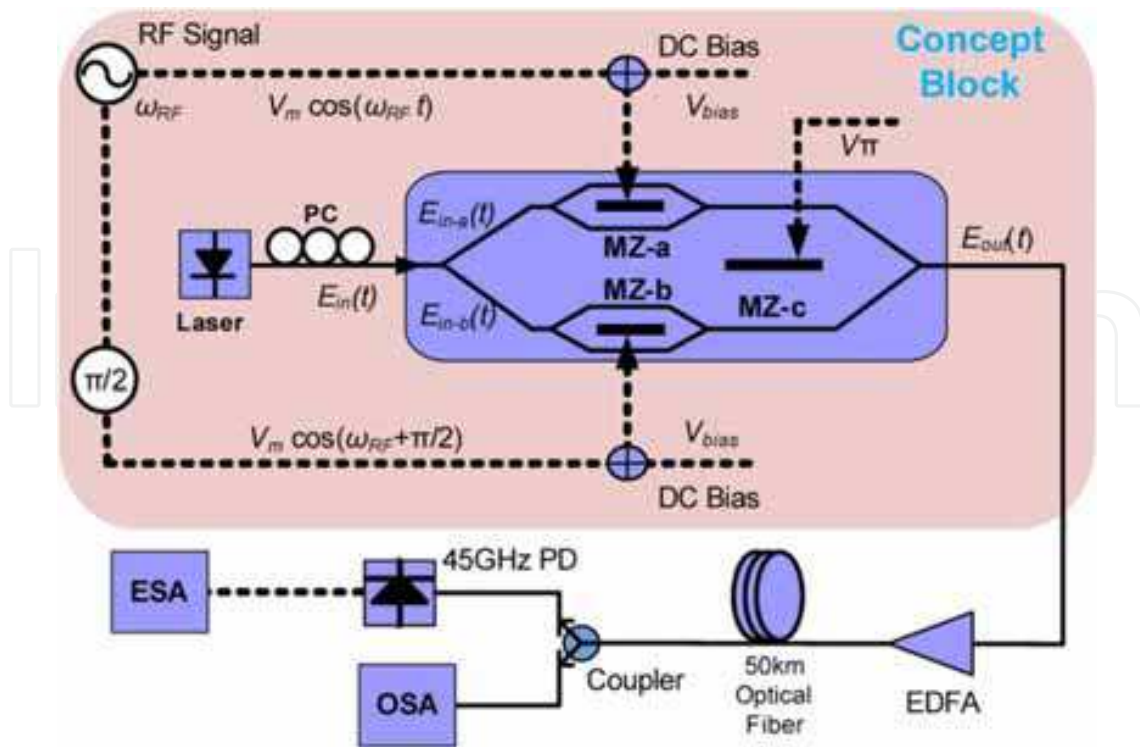


Fig. 12. Optical up-conversion using a frequency multiplication technique for WDM RoF systems. (MZ: Mach-Zehnder modulator; EDFA: erbium-doped fiber amplifier; OSA: optical spectrum analyzer; ESA: electrical spectrum analyzer).

2.6 External phase modulation

In addition to the intensity modulation, external phase modulation is also utilized to produce downstream optical mm-waves in optical-wireless networks. Figure 13 shows the principle of using phase modulator (PM) and subsequent interleaver for mm-wave generation. As a schematic illustration, the case of WDM signals with 100-GHz channel spacing as inset (i) is considered. When the WDM sources are modulated by a PM driven by a 20-GHz sinusoidal RF clock, the signal field of one channel at the output of PM can be written as a few sidebands:

$$E_{output1} = A_s \sum_{n=-\infty}^{+\infty} J_n(m_d) \cos[(\omega_s + n\omega_{RF})t + n\pi/2] \quad (1)$$

where A_s is the amplitude of the original optical carrier, $J_n(m_d)$ is the n^{th} Bessel function of the first kind, $m_d = \pi V_{RF} / V_\pi$ is the modulation depth of PM, V_{RF} is the driving voltage of the RF signals, $n\omega_{RF}$ is the generated sidebands. How many sidebands can be generated depends on the amplitude of the driven RF signal on the PM. Here we assume that only the first-order sideband is generated through optimizing the modulation depth m_d . The peak of the first sideband is 20 GHz away from the original optical carrier as shown as inset (ii). The interleaver, with one input and two out-ports of 25-GHz bandwidth, is used to suppress the optical carrier. When the central wavelengths of the WDM light sources can match up well to the interleaver, the optical carrier of each channel will be suppressed. The output signal of the interleaver is expressed as:

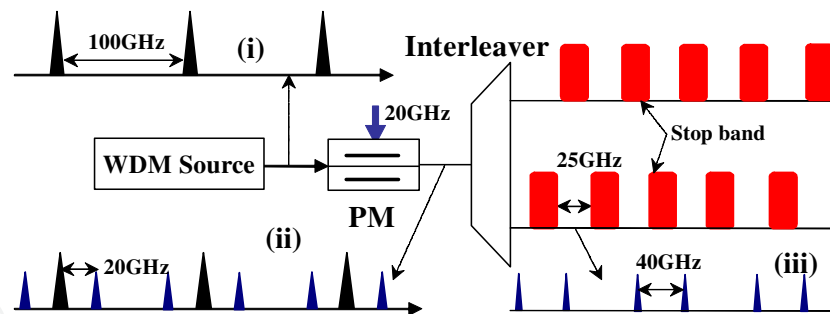


Fig. 13. Concept of using PM and interleaver for mm-wave generation.

$$E_{output2} = A_s \left\{ \sum_{n=-\infty}^{\infty} J_n(m_d) \cos[(\omega_c + n\omega_m)t + n\pi/2] - \alpha J_0(m_d) \cos \omega_c t \right\} \quad (2)$$

where α is the attenuation coefficient of the interleaver filter at the peak of center frequency. The optical spectrum from output 1 of the interleaver is shown in inset (iii). In this way, optical mm-wave WDM channels are generated.

Eight-channel WDM optical mm-wave generation and transmission is demonstrated in one experiment, where eight channel signals at 2.5Gb/s are upconverted into 40GHz mm-wave by a phase modulator and optical filtering technique. Compared optical mm-wave generation by using an intensity modulator, this scheme also exhibits better performance on system stability due to the removal of any DC-bias controller.

3. OFDM-ROF system

In the previous section, all modulation formats for the baseband optical signal are optical On/ Off keying signal. When this optical signal is carried by the optical mm-wave signal at high frequency, the transmission distance of optical mm-wave signals is quite limited by the fiber chromatic dispersion as shown in Fig. 6. On the other hand, orthogonal frequency division multiplexing (OFDM) modulation technology has been widely adopted in ADSL and RF-wireless systems such as IEEE 802.11a/g (Wi-Fi) and IEEE 802.16 (WiMAX). OFDM systems can provide excellent tolerance towards multipath delay spread and frequency-dependent channel distortion. Recently, optical transmission systems employing OFDM have gained considerable research interest because OFDM can overcome the effect of fiber chromatic dispersion and have the capability to use higher level modulation formats to increase spectral efficiency. So the combination of OFDM and ROF is naturally suitable for optical-wireless systems to extend the transmission distance over both fiber and air links.

The first experimental demonstration of a super-broadband OFDM-ROF system based on SCM and interleaver for all-optical mm-wave generation and up-conversion was presented in OFC 2006. In this experiment, the transmission of 4-QAM (QPSK) OFDM analog signals at 1 Gb/s on 40-GHz mm-wave carriers is achieved over 80-km standard single mode fiber (SSMF) without dispersion compensation with less than 0.5-dB power penalty at BER of 10^{-6} . Fig. 14 shows the schematic diagram of mm-wave OFDM-ROF system. At the central office (CO), the OFDM analog data and an RF clock at half of the local oscillator (LO) frequency are mixed by using SCM technology. The mixed signals are applied to drive a LiNbO₃ Mach-Zehnder modulator (LN-MZM) to create first-order sidebands. After transmission over SSMF, an interleaver is employed to separate the optical carrier from the first-order

sidebands to generate optical mm-wave carrier at the BS. Then the boosted electrical mm-wave signal is down-converted through a mixer and retrieved by the OFDM receiver. The separated optical carrier is considered as the continuous wave (CW) and directly modulated by the uplink data and sent back to the CO.

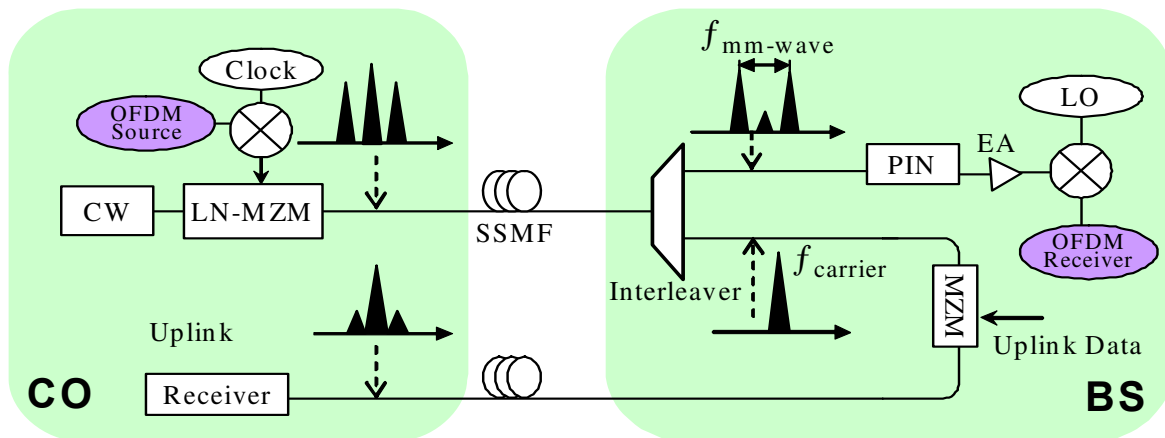


Fig. 14. Architecture of an mm-wave OFDM-ROF system based all-optical up-conversion.

Fig. 15 depicts the experimental setup. At the optical transmitter side, a CW lightwave from a tunable laser (TL) at 1559.7nm (2-MHz linewidth) is modulated by an MZM driven by the mixed OFDM analog signals. The 1-Gb/s OFDM baseband signals are calculated offline with Matlab program including mapping $2^{31}-1$ PRBS into 256 4-QAM-encoded subcarriers, subsequently converting the OFDM symbols into time domain by using IFFT and then adding 6.4-ns cyclic prefix (CP). The digital waveforms are then downloaded to a Tektronix AWG 7102 arbitrary waveform generator (AWG) operating at 10 GS/s to produce 1-Gb/s analog OFDM signals, which is shown in OFDM source in Fig. 15. Among 256 OFDM subcarriers (FFT size), 200 channels are used for data transmission, 55 channels at high frequencies are set to zero for over-sampling, and one channel in the middle of the OFDM spectrum is set to zero for DC in baseband. The output waveforms are shown in Fig. 15 as inset (i). The 1-Gb/s OFDM signals are mixed with a 20-GHz sinusoidal wave to realize SCM for the mm-wave signals and then used to drive the MZM. The electrical spectrum of mixed signals and the optical spectrum of modulated optical signals are shown in Fig. 15 as inset (ii) and (a), respectively. The input power is 14 dBm before transmission over 80-km SSMF. At the optical receiver side, a 50/25-GHz optical interleaver with 35-dB channel isolation and two outputs is used to separate the optical carrier and the sub-carriers. The optical spectra of the separated optical carrier and mm-wave signals are shown in Fig. 15 as (b) and (c), respectively. The carrier is suppressed larger than 20 dB. The optical eye diagram of mm-wave signals is also shown in (b). Regarding the downlink connection, direct detection is made by a 50-GHz bandwidth PIN photodiode. The converted electrical mm-wave signal is then amplified by an electrical amplifier (EA) with 10-GHz bandwidth centered at 40 GHz. A 10-GHz clock is used in combination with a frequency multiplexer to produce 40-GHz electrical LO signal later mixed to down-convert the electrical signal to OFDM baseband form. The down-converted signals are sampled with a real-time digital oscilloscope (Tektronix TDS6154C). The received data are processed and recovered off-line with a Matlab program as an OFDM receiver. The sampling frequency is 1.25 GHz. The electrical spectrum of down-converted OFDM signals is shown in Fig. 15 as (iii). The

spectrum fluctuations for different frequency components arise from the nonlinear response of TL, MZM and optical amplifier due to the large optical power. The measured power penalty for the downstream optical signal is smaller than 2dB.

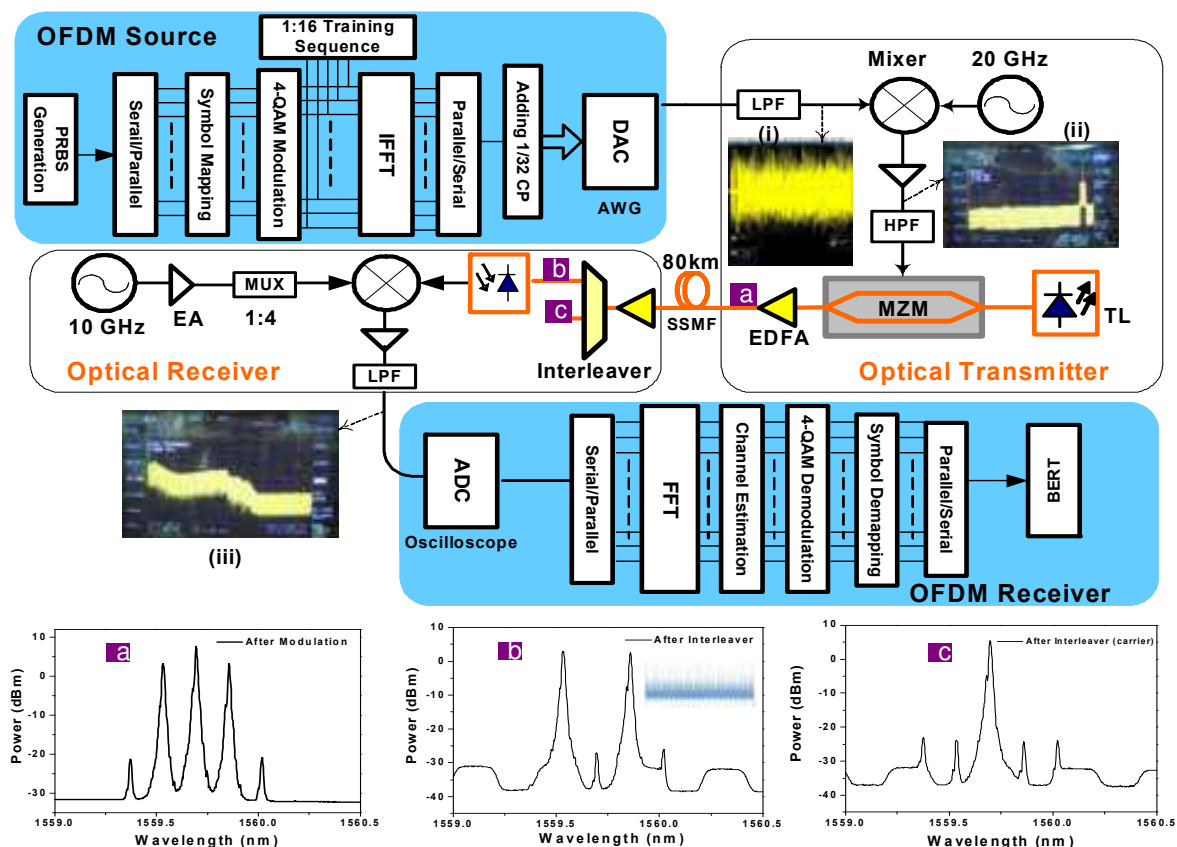


Fig. 15. Experimental setup for OFDM-ROF systems transmission over 80-km SSMF at 1Gb/s on 40-GHz mm-wave carrier. The electrical waveform and spectra are inserted. The optical spectra measured at point a, b, c are all inserted. The resolution for optical spectra is 0.01nm.

Usually, OFDM signal has a high peak to average power ratio (PAPR), and this high PAPR limits the transmission distance of optical OFDM. The PAPR of the optical OFDM can be reduced when the optical OFDM signal is generated by phase modulator because of its constant intensity of the optical OFDM signal. Recent experiment has confirmed this conclusion. In addition, advanced coding technique can be used to improve the receive sensitivity of the optical OFDM signal.

Figure 16 shows the principle of the OFDM-ROF architecture based on optical mm-wave signal generation by a phase modulator and turbo coding technique. The original data is encoded by turbo coding technique and then modulated in an OFDM block based on IFFT. The OFDM signal after mixing with the LO clock signal is used to drive a phase modulator to modulate lightwave from a CW lightwave source and generate optical mm-wave. Different kinds of signals have different PAPR. For example, OOK NRZ signal has a PAPR of 3dB, and OFDM intensity optical signal has more than 10dB. To reduce PAPR, one employs phase modulator for its constant amplitude. Comparing with the OFDM signal generated by an intensity modulator, optical OFDM signal generated by a phase modulator

has two other benefits: 1) high OSNR due to relatively small insertion loss of a phase modulator, and 2) high stability without dc bias control system. Using advanced coding technique the receiver sensitivity can be improved over 2dB in the recent experiment.

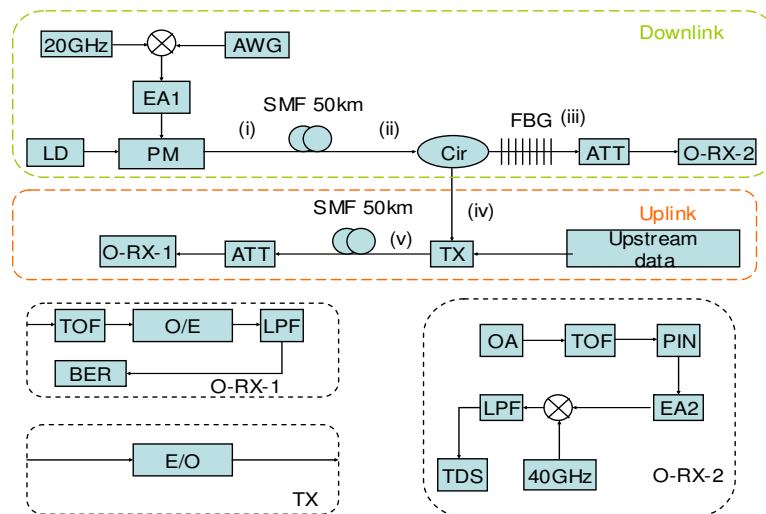


Fig. 16. Experimental setup of OFDM-RoF architecture based on phase modulator. AWG: arbitrary waveform generator, PM: phase modulator, EA: electrical amplifier, FBG: fiber Bragg grating, ATT: attenuator, O-RX: optical receiver, TX: transmitter, TOF: tunable optical fiber, LPF: low pass filter, BER: bit error tester, OA: optical amplifier, TDS: time domain scope (real time Osc.), O/ E: optical/ electrical converter, E/ O: electrical/ optical converter.

The experimental setup is depicted in Fig. 17. The center wavelength of the continuous lightwave (CW) generated by a distributed feedback laser-diode (DFB-LD) is 1543.72nm. The RF signal is generated by an electrical mixer to combine the 20GHz RF clock (sinusoidal wave) and 2.5-Gb/ s OFDM signals. Then the mixed electrical signals are boosted to drive the phase modulator as shown in Fig. 16. The waveform and spectrum of OFDM source is depicted as inset (a) and (b) in Fig.16, respectively. In this experiment, the OFDM signal based on QPSK I/ Q modulation scheme is generated by the Tektronix arbitrary waveform generator. Original data is encoded by recursive systematic convolution code (RSC1) firstly, and combine the interleaving original signal after RSC2. The length of interleaving is 1024. The generator vector of RSC is $g_0 = (1, 0, 11; 1101)$. RSC encoding rate is 1/ 2. Then the combining data is punctured. Combining the original OFDM signal and puncturing data, encoding data is generated and modulated in the way of OFDM modulation. The Turbo coding rate is 2/ 3. In the OFDM frame there are 256 subcarriers, among them, 200 subcarriers are used for data and 56 subcarriers are set to zero as guard interval. The guard interval (cyclic prefix) in time domain is 1/ 32 which would be eight symbols every OFDM frame. The first and second order sideband is 20 and 50dB smaller than the carrier, respectively. The input power into transmission fiber is 13.2dBm. After 50-km SMF-28, the optical signals are divided into two parts including central optical carrier and two first order sidebands by a fiber Bragg grating (FBG) as depicted in Fig.16. The FBG is used to remove the central carrier and converted phase to intensity signals. An optical receiver (OR2) contains an EDFA as preamplifier and an optical band-pass filter (OBPF) with the 3dB

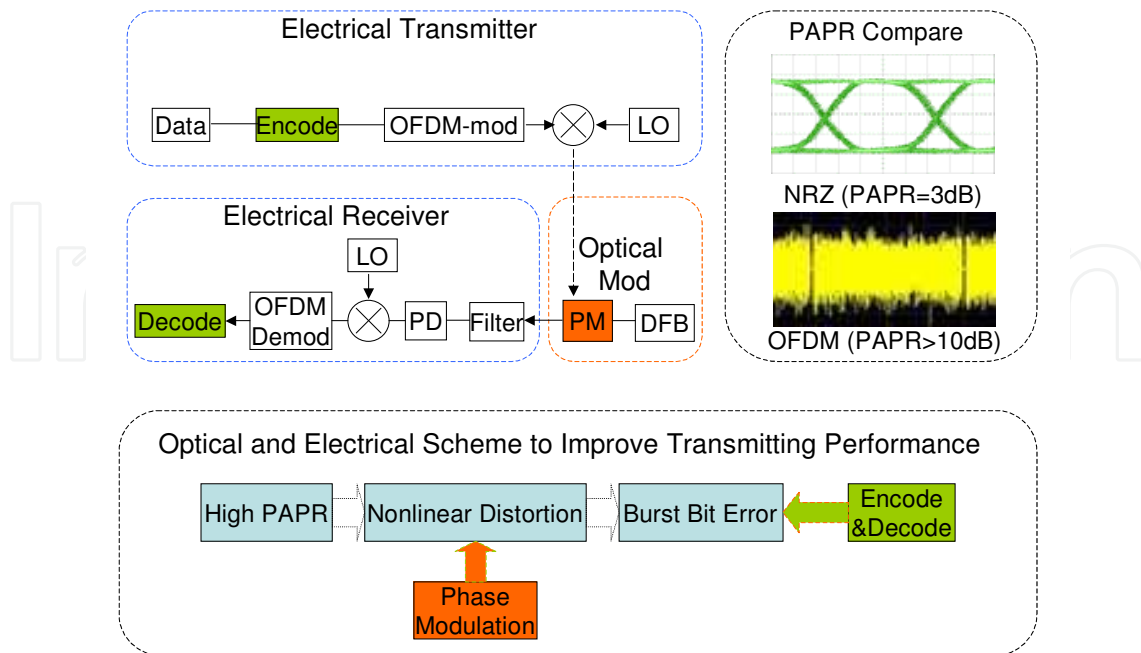


Fig. 17. Principle of the OFDM-ROF architecture based on a phase modulator with channel coding. Encode: Turbo encoding, LO: local oscillator, DFB: distributed feedback laser diode, PM: phase modulator, PD: photo-detector, Decode: Turbo decoding.

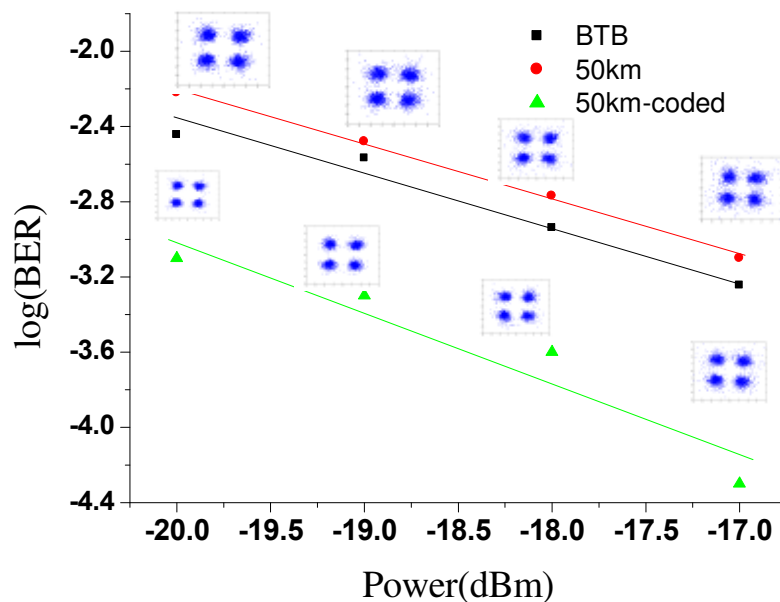


Fig. 18. BER curves for down-link OFDM optical signal.

bandwidth of 1nm as ASE noise block, respectively. Then the optical OFDM signals are converted to electrical signals by a PIN with the 3dB bandwidth of 50 GHz. After that, the converted electrical signals are down-converted to the baseband and sampled by a

Tektronix real-time oscilloscope and processed off-line. The center carrier is re-modulated by intensity modulator (IM) driven by 2.5Gb/s uplink PRBS data with a word length of $2^{31}-1$. The received constellations of the OFDM signals before and after transmission over 50km downlink SMF-28 and the corresponding BER performance are shown in Fig. 18. A little expansion in the received constellation comes from the OSNR degradation. OFDM signals before and after transmission at a BER of 1×10^{-3} is -17.62 and -17.25 dBm. For upstream optical signal at 2.5Gb/s, there is no power penalty after transmission over 50km upstream fiber because the effect of the dispersion of 50km SMF-28 on the 2.5Gbit/s signals is very small.

4. Seamless integration of ROF with WDM-PON

Wavelength division multiplexed passive optical network (WDM-PON) has been regarded as a promising solution to meet access bandwidth requirements for delivering gigabits/sec data and video services to large number of users. The design of WDM-PON architecture is expected to be compatible with radio-over-fiber system without any change of optical line terminal (OLT) configuration to flexibly serve both fixed and mobile users. Here, we show two different architectures to realize this function of seamless integration of ROF with WDM-PON.

The first architecture is based on subcarrier multiplexing (SCM) technology to generate optical mm-wave signal and provide the lightwave source for up-stream reuse in WDM-PON network. The commercially available package of integrated SOA and EAM is used to be the uplink transmitter to increase the power margin through eliminating the need of RSOA and external modulators. Based on this scheme, the symmetric 2.5Gbit/s data signals per channel are transmitted over the same 40km single mode fiber (SMF) for both directions with less than 1dB power penalty.

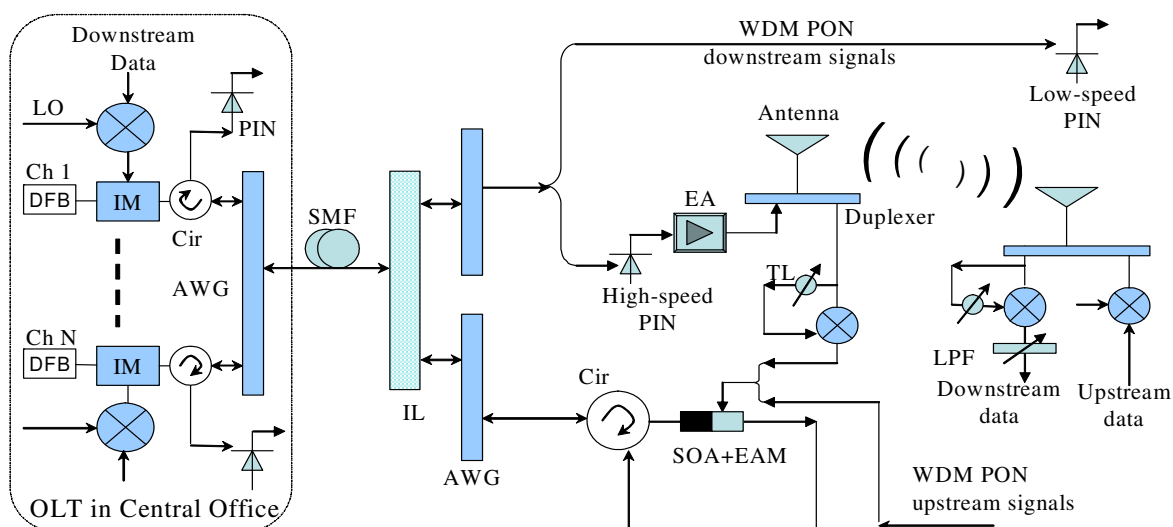


Fig. 19. WDM-PON access network compatible with ROF system. IL: interleaver, Cir: circulator, LPF: low-pass filter, TL: tunable line delay, IM: intensity modulator.

The network configuration is shown in Fig. 19. Each laser is modulated by means of SCM technique. A broadband downstream data after mixing with the LO clock signal are used to

directly or externally modulate the lightwave. The WDM SCM signals are multiplexed by using an AWG before they are sent to the ONU after transmission over fiber. In the ONU or base-station, the WDM SCM signals are passed through an optical interleaver to realize the separation of the optical carrier and subcarrier signals where DI-MZ interferometer was employed. The optical interleaver has higher optical carrier suppression ratio and adjacent channel isolation compared to the DI-MZ interferometer. The separated optical carrier is then passed an AWG and delivered to the customer unit or base station before re-modulation by using an integrated SOA and EAM. Here SOA is used to provide the gain. Then the modulated upstream optical signals will be sent back to the OLT or central office after transmission over the same transmission fiber of the downstream signals before they detected by a 3R receiver.

For regular WDM-PON application, the separated subcarrier signals after AWG will be detected by a low-speed photo-diode before 3R receiver. For wireless service provided by ROF, the subcarrier signals are broadcasted by an antenna before detection by a high-speed receiver and amplification by a narrow-band electrical amplifier EA. At the customer unit, the wireless signal is received by an antenna and down-converted by a mixer to retrieve the baseband signals. For wireless upstream, the up-converted data will be sent back to the base station by wireless transmission. After amplification and down-conversion, it will modulate the EAM before it is sent back to the central office. In this scheme, we do not need to change the OLT configuration to make the WDM-PON compatible with ROF network.

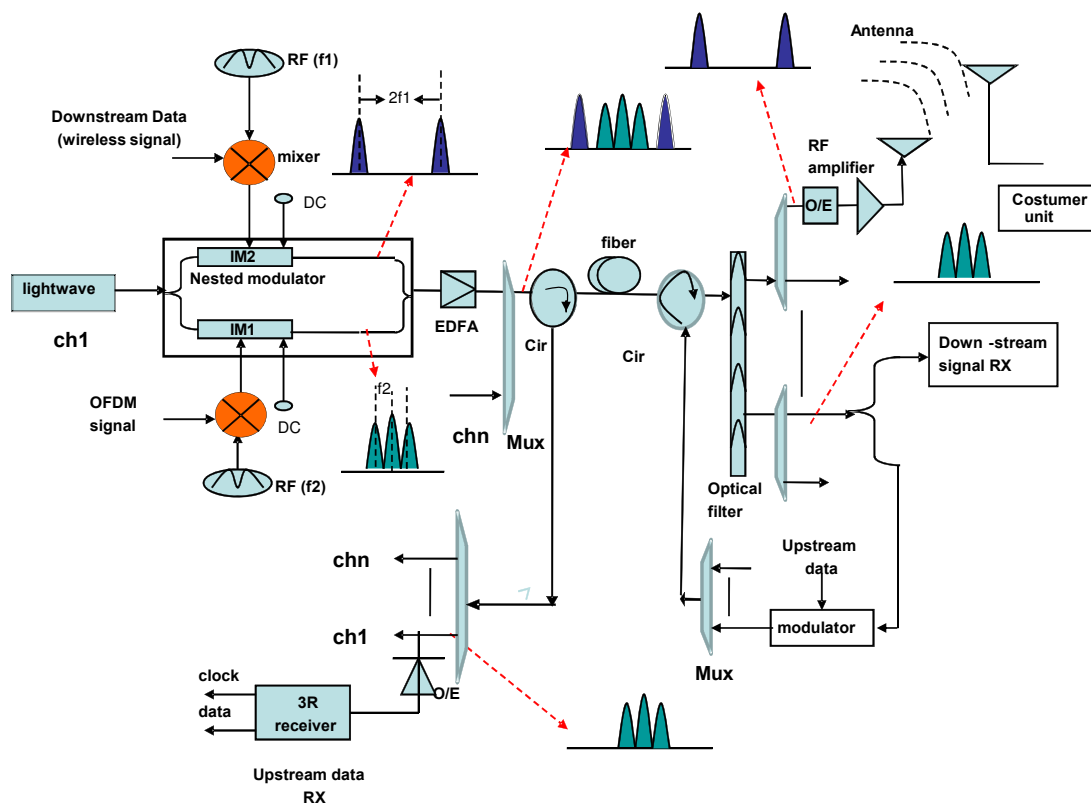


Fig. 20. Schematic diagram of the seamless integration of ROF with WDM-PON for providing triple service.

Other architecture is based on an external integrated modulator to generate optical mm-wave and provide lightwave for upstream reuse. Since the two arms in the integrated modulator do not affect each other, the generated mm-wave signal and the baseband optical signal have higher quality.

The proposed novel WDM-PON architecture is shown in Fig. 20. The CW lightwave is modulated by an external integrated modulator using x-cut LiNbO₃, consisting of two single-electrode Mach-Zehnder modulators (MZMs). The separated lightwave in the integrated modulator is modulated by intensity modulator (IM) IM-1 and IM-2 to generate SCM signal, respectively. The optical mm-wave is generated based on OCS modulation to carry the wireless signal by IM-1 while OFDM wired signal is based on DSB modulation by IM-2. The IM-1 and IM-2 has a 90 degree phase shift to avoid the interference between the up and bottom optical signal, hence there is no crosstalk between the mm-wave and baseband signal. The wireless signal and wired signal are combined by a waveguide coupler before all channels are multiplexed. After transmission over the optical fiber, a fiber filter is used to separate the OCS modulated downstream wireless signals and the double sideband (DSB) modulated downstream wired OFDM signals. The OCS modulated wireless downstream signals at different wavelengths are demultiplexed to the customer unit by antenna before the O/E conversion. The DSB modulated downstream wired signals, after being demultiplexed, are sent to two paths. One part is converted to electrical OFDM wired signal by a low speed receiver. The other part is re-modulated by an IM driven by the upstream data. The WDM upstream data are demultiplexed before they are O/E converted.

5. Wavelength reuse for upstream

It has been expected that mm-wave bands would be utilized to meet the requirement for high bandwidth and overcome the frequency congestion in the optical-wireless networks. The negative side of mm-waves is the need for numerous BSs, which is a consequence of high RF propagation losses in the atmosphere. In this situation, it is necessary to minimize the cost of the BS and shift the system complexity and expensive devices to the CO. Hence, the overall architecture design and the scheme of RF signal generation, transmission for the uplink and downlink play the key roles on the successful deployment in the real networks. Fig. 21 shows two ROF systems with downstream and upstream connection. In Fig. 21(a), it shows a simple ROF system. The CW lightwave is modulated for up-conversion to generate optical mm-wave signal. The optical mm-wave signal is delivered to the base station by optical fiber. The optical fiber can be standard single mode fiber for long distance (>1km) transmission or multi-mode fiber for short distance transmission. The fiber loss can be compensated by optical amplifier. In the base station, the optical mm-wave signal is detected by a high-speed photodiode. Then the electrical mm-wave signal is boosted by a narrow-band electrical amplifier (EA) before it is broadcasted by antenna to the customer unit. The electrical upstream data obtained from the antenna is boosted by a narrow band EA. The boosted electrical upstream signal is used to drive an external modulator such as intensity modulator, electro-absorption modulator (EAM). The CW lightwave for upstream connection is generated from a lightwave source. The generated upstream mm-wave signal is delivered to the central office by upstream fiber. The upstream fiber and downstream can be the same fiber, however, it may have crosstalk between them. Obviously, in this architecture, an additional CW lightwave source is necessary at the base station. To simplify the base station, we can use the architecture shown in Fig. 21(b). Here the CW lightwave for

upstream connection is extracted from the downstream optical signals. It means that a part of downstream signal is reused. This is quite similar to that technique used in WDM-PON architecture with source-free at remote node. For uplink connection, some methods have been recently proposed. However, most of them only demonstrated uplink connections over short transmission distances. Full-duplex operation using high RF carrier still raises difficulties that have to be addressed. The network architecture consisting in a single light source at the CO and the reuse of the downlink wavelength at the BS is an attractive solution for low-cost implementation as it requires no additional light source and wavelength management at the BS.

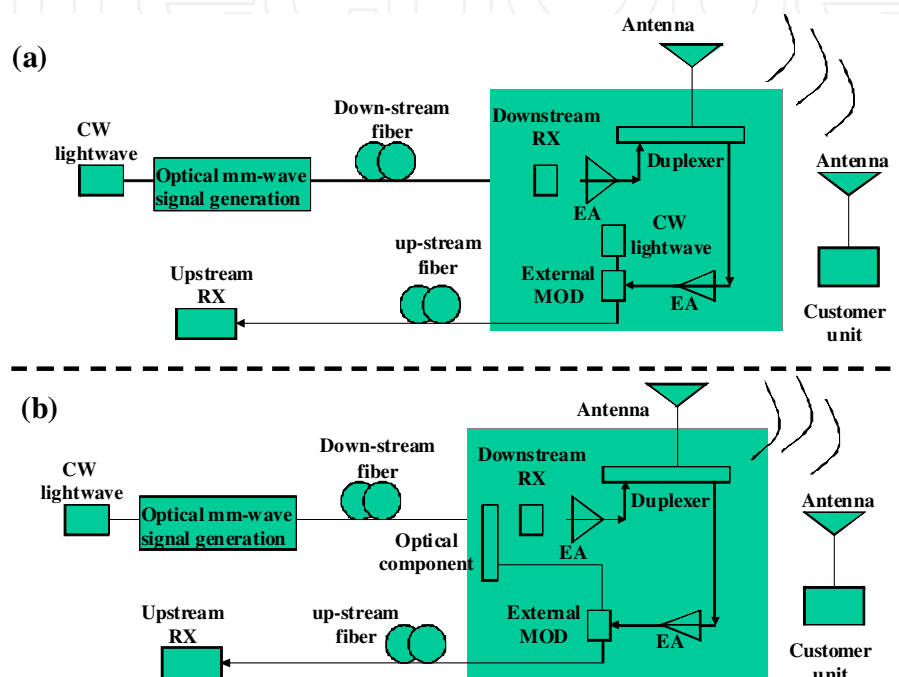


Fig. 21. ROF system with downstream and upstream connection.

5.1 IM with subsequent filter for downstream and OOK upstream generated by an external modulator

Figure 22 shows the principle to generate optical mm-wave by using DSB modulation along with optical filtering, and wavelength reuse for uplink connection. An external modulator such as LiNbO_3 modulator or electro-absorption modulator driven by RF signal can be used to generate DSB modulation signal. Usually the first and second sidebands will be generated after modulation. Here one can use an optical interleaver to separate the first order sideband from the optical carrier and the second order sideband signals. The two peak modes of the first order sideband will be beat to generate an optical mm-wave with a double repetitive frequency of the RF signal when they are detected by an optical receiver. The baseband down-link data is added on the optical mm-wave by using additional external intensity modulator. The separated optical carrier and the second order sideband signals are further separated by the second interleaver. After this, we can obtain a pure optical carrier. The pure optical carrier will be combined with the downlink optical mm-wave signal by using a 3dB optical coupler. In the base station, we use the third optical interleaver to separate the downlink optical mm-wave and the pure optical carrier. The separated downlink optical mm-wave signal is received by a high-speed detector, then, it is boosted by a narrow-band

electrical amplifier before it is broadcasted by an antenna. The received uplink data from the antenna firstly are down-converted by using an electrical mixer. The down-conversion can be realized by using an electrical mixer without LO. The baseband uplink data is used to drive an external modulator to generate optical uplink data before it is transmitted over the fiber to reach the central office. Since the optical interleaver has periodic characteristic, this scheme for this ROF architecture including optical mm-wave generation and wavelength reuse for uplink connection can be used to generate the DWDM optical mm-wave and deliver them by sharing the same interleavers.

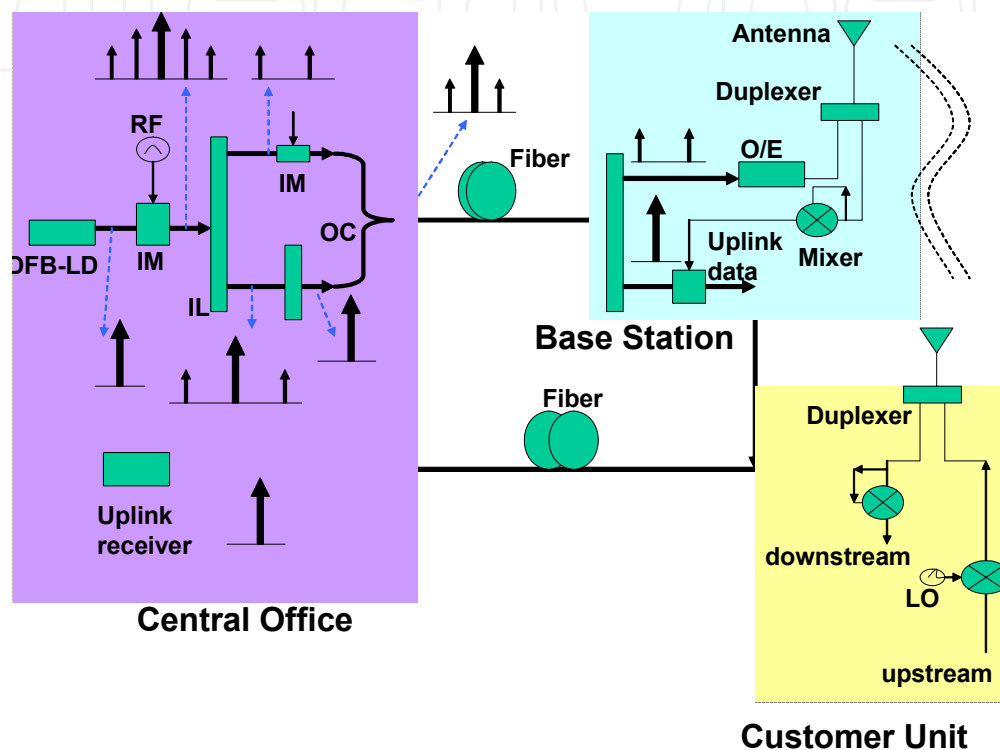


Fig. 22. Principle of DWDM optical mm-wave generation using phase modulator and optical interleaver. IL: Interleaver, IM: intensity modulator, OC: optical coupler, O/ E: optical/ electrical converter, LO: local oscillator.

In real network implementations, the diplexer connected with the antenna would act as a circulator to handle the up- and down-stream signals at the BS. The baseband upstream signals would be obtained after down-conversion of the end user's information coming from the diplexer in the BS. In this experiment, the same fiber length is used for both up-and down-streams. The uplink signal is detected by a low-frequency response receiver which also filters out the residual part of mm-wave signals.

5.2 OCS for downstream and reuse for upstream

The schematic diagram is shown in Fig. 23. OCS scheme is employed to generate optical mm-wave and up-convert baseband data signal simultaneously for the downstream. The original carrier is split prior to OCS operation and then coupled with optical mm-wave signal before they are transmitted to the BS. At the BS, a fiber Bragg grating (FBG) is used to reflect the carrier while passing the optical mm-wave signal to downlink receiver. The reflected carrier is acted as the CW and re-modulated with the symmetric upstream signal,

then transmitted back to CO, where a low-cost receiver with low-frequency response detects the upstream signal.

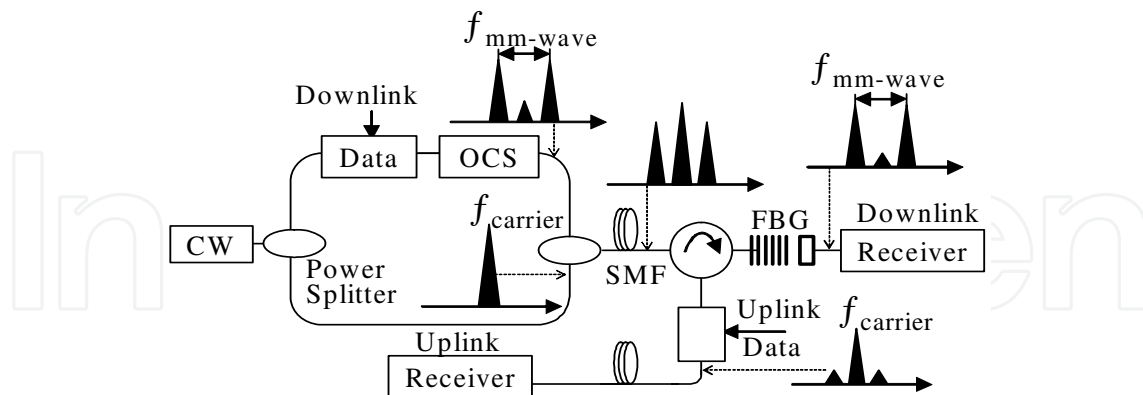


Fig. 23. A full-duplex ROF system based on OCS and reuse.

The experimental setup for the full-duplex ROF system is shown in Fig. 24. At the CS, a CW is generated by a TL at 1549.1 nm and split into two parts via a 50:50 optical PS. The first part is modulated via an M-Z modulator driven by 2.5-Gb/s signals. Optical mm-wave signals are generated by using OCS scheme. The optical spectrum and eye diagram after OCS are measured at point A, B and inset (i), (ii) in Fig. 24, respectively. Then the generated optical mm-wave is amplified by an EDFA to get a power of 6 dBm for transmission. The second part is sent directly for amplification by an EDFA to obtain a power of 9 dBm and then combined with the first part via OC before they are transmitted over SMF.

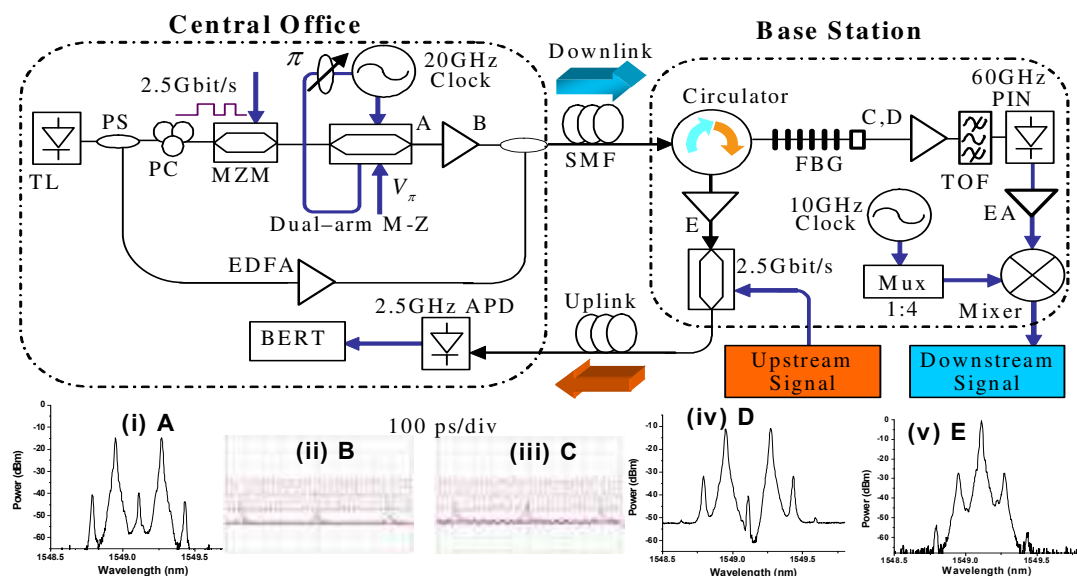


Fig. 24. Experimental setup for full-duplex ROF system based on optical carrier suppression and reuse.

At the BS, the FBG is used to take on two roles: one is to reflect the optical carrier to provide CW light source for uplink connection; the other is to pass the two sidebands generated by OCS simultaneously and as a consequence, it increased the carrier suppression ratio up to 30 dB due to sharp notch characteristics. This FBG filter has a 3-dB reflection bandwidth of 0.2 nm and reflection ratio larger than 50 dB at the reflection peak wavelength. The eye

diagram, the spectrum of passing part and reflected part are measured at point C, D, E and inset (iii), (iv) and (v) in Fig.24. Then we use the identical O/ E and down-conversion to retrieve the downstream signals. Fig. 25 shows that the evolution of dispersion impact on different distances for two directions signals. It is clearly seen that the eye still keeps open in despite of transmission over 40-km SMF, which is long enough for access network coverage. But the uplink might transmit longer distance because most of the component of high frequency is removed already by FBG filter before it is sent back to the CO. For the uplink, the reflected signal is amplified by an EDFA to compensate the insertion loss of the filter before it is modulated by symmetric 2.5-Gb/ s electrical signal.

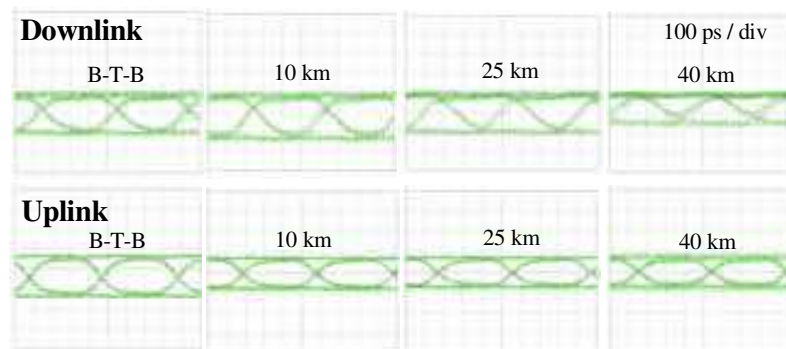


Fig. 25. Electrical eye diagrams after different length transmission.

5.3 PM with subsequent filter for downstream and directly modulated SOA for upstream

Fig. 26 shows the schematic diagram of full-duplex optical-wireless system architecture by using PM and SOA. An optical PM is driven by small RF signal ($1/4$ half-wave voltage of the PM) to create first-order sidebands while suppress the second-order components for increasing dispersion tolerance. An interleaver is employed to separate the optical carrier from the first-order sidebands to generate optical mm-wave carrier. After modulation by downlink data, the up-converted optical signal is combined with the original optical carrier and transmitted over the SMF. At the BS, an FBG is used to reflect the optical carrier while pass the optical mm-wave signal to O/ E conversion. Then, the boosted electrical mm-wave signal is broadcasted by an antenna through a duplexer acting as a circulator to handle up- and down-stream signals at the BS. On the other hand, the upstream signals are down-converted through a mixer and tunable delay (TD) line without the need of LO signal.

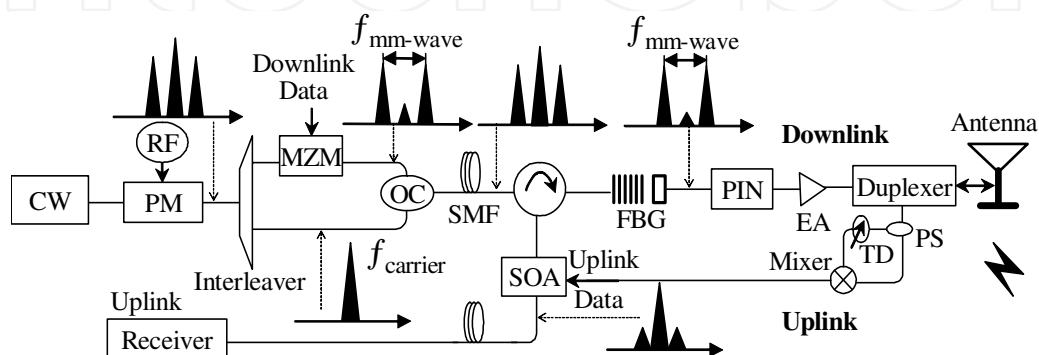


Fig. 26. Architecture of a full-duplex optical-wireless system by using PM and SOA.

The reflected optical carrier is considered as the CW source and directly modulated by baseband upstream signals in the SOA and sent back to the CS, where a low-cost and low-frequency response receiver is used for detection. In this scheme, the SOA performs the function of both amplification and modulation, which eliminates the requirement of optical amplifier and external modulator at the BS.

Fig. 27 depicts the experiment setup for the full-duplex optical-wireless system by using wavelength reuse and directly modulated SOA. At the CO, A CW is generated by a DFB-LD at 1534.4 nm and modulated by an optical PM driven by a 20-GHz RF sinusoidal wave with amplitude 1 V (half-wave voltage of the PM is 4 V). The optical spectrum (measured at point a) after modulation is shown in Fig. 27 as inset (a). A 50/ 25-GHz optical interleaver with 35-dB channel isolation is used to separate the remained optical carrier from the first-order sidebands. The generated optical mm-wave is then amplified and modulated by an IM driven by 2.5-Gb/ s PRBS $2^{31}-1$ electrical downstream signals. The separated optical carrier is directly sent to combine with up-converted baseband signals via OC before its transmission over 40-km SMF-28 with 8-dBm input power. The optical spectra of the separated optical carrier, optical mm-wave signal and combined signals are shown in Fig. 27 as inset (b), inset (c) and inset (d), respectively. At the BS, a FBG is used to reflect the optical carrier and transmit the optical mm-wave signals simultaneously. The FBG filter has a 3 dB reflection bandwidth of 0.2 nm and reflection ratio larger than 50 dB at the reflection peak wavelength. The spectra of reflected carrier and transmitted optical mm-wave signals are shown in Fig. 26 as inset (e) and inset (f). The downstream signals are down-converted through a mixer and TD line without requiring any LO signal.

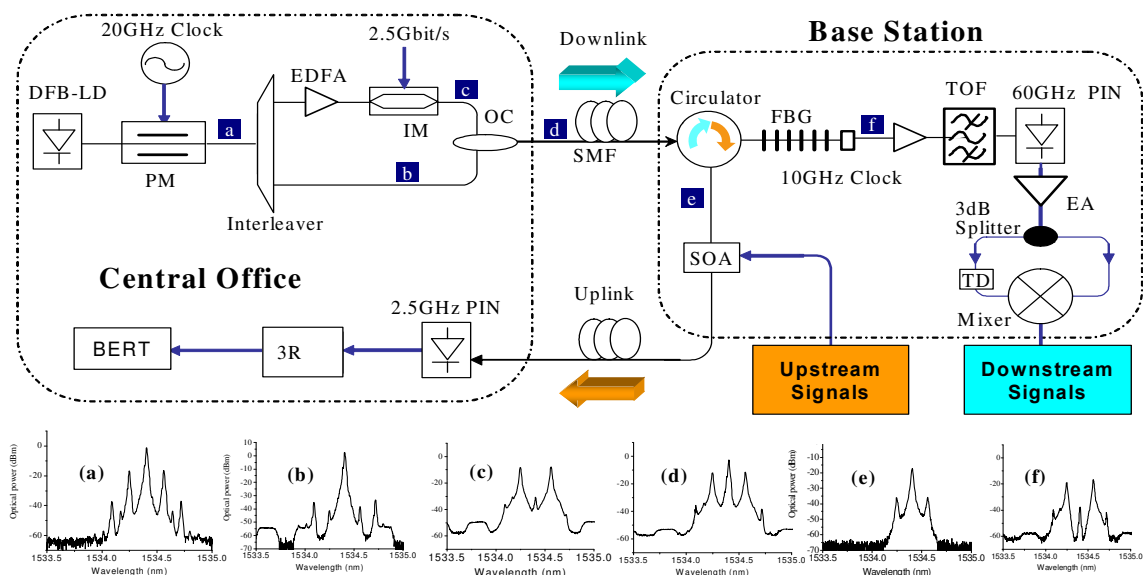


Fig. 27. Experimental setup for the full-duplex optical-wireless system by using wavelength reuse and directly modulated SOA. The optical spectra measured at point a, b, c, d, e, f are all inserted as insets.

For the uplink, the reflected optical carrier is directly modulated in an SOA driven by a 250-Mb/ s (PRBS 2^7-1) electrical signal with amplitude 3.1-V and 165-mA bias. The gain is 10 dB in the 34-nm spectral width and the polarization sensitivity is smaller than 0.5 dB. In this experiment, the same fiber length is used for both up- and down-streams. The uplink signal

is detected by a low-frequency response receiver which also filters out the residual part of the high-frequency mm-wave signal due to imperfect filtering by the FBG.

Fig. 28 shows the optical eye diagrams in B-T-B configuration and after the 40 km propagation in the SMF. The power fluctuations of the 40-GHz modulation arise from the chromatic dispersion in the fiber. The power penalty is measured. For the downlink, the power penalty at the given BER of 10^{-10} is 2.0 dB after 40-km transmission. For the uplink, the power penalty for the re-modulated optical carrier is around 0.5 dB over the same transmission distance. The eye diagrams of B-T-B configuration for both directions are also inserted in Fig. 28.

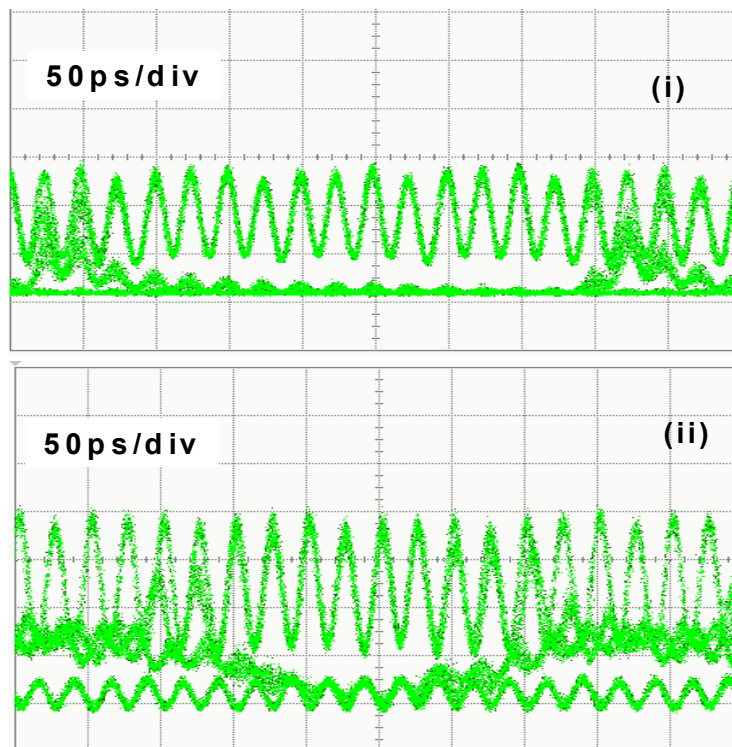


Fig. 28. Optical eye diagrams for downstream signals at (i) B-T-B and (ii) after 40km transmission.

5.4 Integrated modulator for optical mm-wave and baseband generation and wavelength reuse

The experimental setup for integrated 60-GHz bidirectional ROF and WDM-PON system using a single I/Q (nested) modulator is shown in Fig.28. At the central office, a CW lightwave is generated by a tunable laser (TL) at 1557.1nm. The I/Q modulator integrates two intensity Mach-Zehnder modulators and a phase shifter. The intensity modulator at the upper arm is driven by 10-Gb/s electrical signals with $2V_{\pi}$ (half-wave voltage of 5V) and PRBS length of $2^{31}-1$. The modulator is biased at the null point to generate phase modulated optical signal (DPSK signal). The intensity modulator at the bottom arm is driven by a RF signal mixed with 30-GHz clock and 2.5-Gb/s baseband signal with the same PRBS length. This modulator is also biased at the null point. Through adjusting the DC bias on the phase shifter, we generate 90 degree phase difference between the upper and bottom arm optical signal. In this way, coherent crosstalk is reduced between the two arms. Optical signals are

then boosted to 16 dBm before they are launched into the 20-km standard SMF-28. The optical spectrum before the EDFA is shown in Fig. 29 inset (a). After transmission, a 25-GHz optical interleaver is used to separate the optical wired signals (baseband signals) from the wireless signals (60-GHz optical mm-wave). The optical spectra of the two output ports of the IL are shown in Fig. 29 insets (b) and (d). The wired optical signal is divided into two parts. One is detected by a standard DPSK balanced receiver. Another part is reused for upstream connection. The eye diagram of this downstream DPSK signal at the BS is shown in Fig. 29 inset (i). Another 50-GHz optical interleaver is employed to further suppress wired signal as shown in inset (c). The 60-GHz optical mm-wave signals are pre-amplified by a regular EDFA with a small-signal gain of 30 dB, and then filtered by a tunable optical filter (TOF) with the bandwidth of 0.8 nm to suppress ASE noise before O/E conversion via a PIN PD with a 3-dB bandwidth of 60 GHz. The converted electrical signal is then amplified by an electrical amplifier (EA) with a bandwidth of 10 GHz centered at 60 GHz. An electrical LO signal at 60 GHz is generated by using a frequency multiplier from 15- to 60-GHz. We use the electrical LO signal and an electrical mixer to down-convert the electrical mm-wave signal to the baseband. The optical eye diagrams of the 60-GHz optical mm-wave signals before and after down-conversion are shown in Fig. 29. The power penalty is negligible at a BER of 1×10^{-10} . The wired BPSK optical signals are detected by a standard balanced receiver, which includes a one bit M-Z delay interferometer (MZ-DI, demodulator) and a balanced detector. There is no power penalty after transmission over

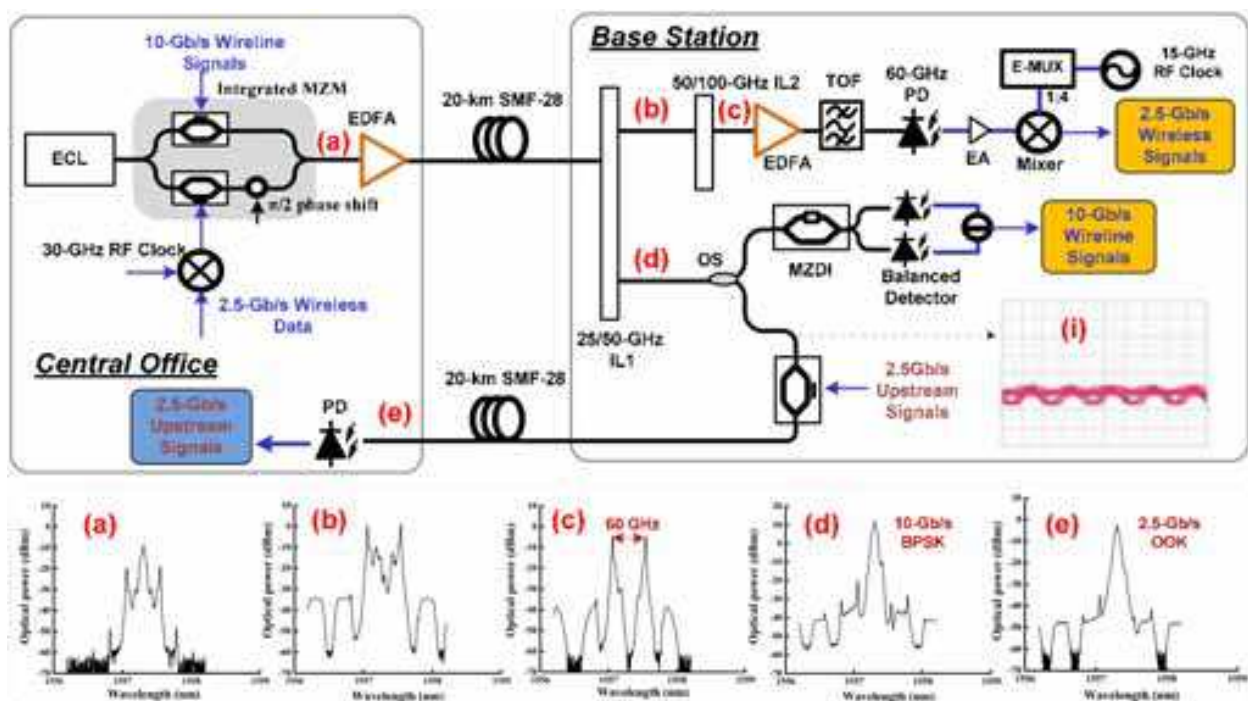


Fig. 29. Experimental setup. ECL: external cavity laser, MZM: Mach Zehnder modulator, IL: interleaver, TOF: tunable optical filter, EA: electrical amplifier, OS: optical splitter, MZDI: Mach Zehnder delay interferometer, resolution: 0.01nm.

20-km SSMF-28. The optical DPSK signal is re-modulated for upstream reuse by one intensity modulator driven by symmetric 2.5-Gb/s PRBS electrical signals with a word length of $2^{31}-1$. In real networks, the diplexer connected with the antenna would be used to circulate the transmitting and receiving signal at the BS. The baseband upstream signals will be obtained after down-conversion of end user's information coming from the diplexer in the BS. In this experiment, after transmission over the same length SMF-28 as the downlink channel, the upstream optical signals are detected by a commercial APD receiver. The optical spectrum of the upstream optical signal after transmission over 20-km uplink fiber is shown in Fig. 29(e). The eye diagrams of optical upstream signals are shown in Fig. 30. Fig. 30 (e) is detected by a 60-GHz photodiode, in which the transit peak of the downstream DPSK signal exists. After detected by a 2-GHz photodiode, the transit peak of DPSK signal is removed as Fig. 30(f). Negligible power penalty is observed after transmission for the upstream signal.

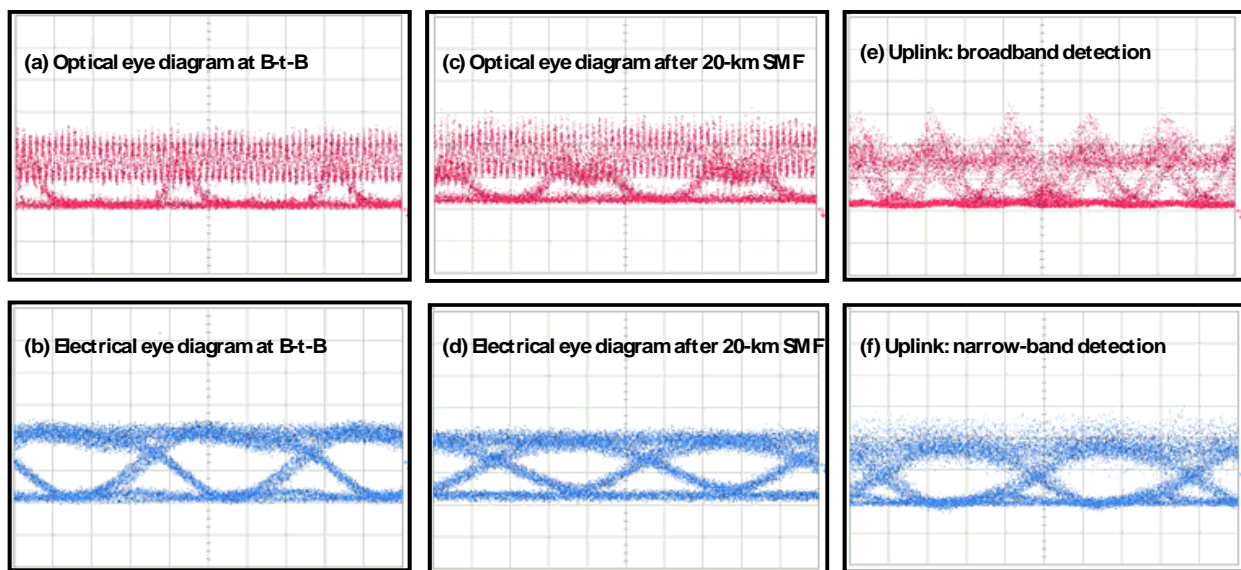


Fig. 30. Measured eye diagrams of downstream (a-d) and upstream (e-f) over 20-km SMF-28.

6. Optical OFDM signals over GI-POF

Perfluorinated graded-index polymer optical fibers (GI-POFs) can provide large bandwidth and low attenuation (60dB/km) at 850–1300nm, so it is a good replacement and a low cost alternative to traditional glass. With ease of use and affordability, GI-POFs make an excellent choice for the installation of high performance fiber networks. In addition, GI-POFs provide a higher transmission bandwidth than any other type of plastic optical fiber. Recently, a few 40Gb/s transmission experiments have been demonstrated. Until recently, all commercially available POFs have been fabricated from non-fluorinated polymers such as PMMA and, as a result, have had a refractive index that changes in steps. Although inexpensive, these fibers are characterized by large modal dispersion and typically operate at 530nm or 650nm, which is well outside of standard communication wavelengths (850nm or 1300nm), which is where high-speed transceivers are readily available. Due to the high attenuation in the near infrared, these fibers are restricted to low performance (<100Mb/s), short range (<50m) applications in the visible region. With the advent of an amorphous perfluorinated polymer, polyperfluoro-butenylvinylether (commercially known as

CYTOP®), the limitations presented by step-index POFs have been overcome. Perfluorinated fiber exhibits very low attenuation in the near infrared (~10dB/ km) as shown in Fig. 5. Moreover, since the perfluorinated optical fiber can be constructed with a graded refractive index, it is capable of supporting bandwidths that are 100 times larger than those provided by conventional POFs. This is due to the interplay between high mode coupling, low material dispersion, and differential mode attenuation. Unlike conventional glass fibers, which suffer from high interconnection and receiver costs, perfluorinated GI-POFs are easy to install. To add a connector to a glass fiber, the fiber needs to be cleaved using an expensive, specialized tool. Then, epoxy is used to attach the fiber to the connector hardware. Finally, the assembled connector must be polished. In contrast, the GI-POF can be terminated using simple and inexpensive tools, connectors are crimped on, and polishing occurs in mere seconds, leading to a high quality optical link in a fraction of the time. Moreover, GI-POFs are compatible with standard multimode glass fiber transceivers. As an example, Table 2 lists the specification of the commercial GI-POF from Thorlabs.

Since 2006, a few world records by employing GI-POF have been achieved. The optical fiber communication conference (OFC) 2006, Georgia Tech's researchers reported that 30Gb/ s on/ off keying (OOK) signals are transmitted over 30m GI-POF. In ECOC 2007, Schollmann et al., reported the 40Gb/ s OOK signals are delivered over 50m GI-POF with new designed multi-mode high-speed receiver. In OFC 2008, Yu in NEC Labs America reported 42.8Gb/ s optical signal generated by chirped managed laser transmission over 100m GI-POF. In ECOC 2008, Yu in NEC Labs America demonstrated 16Gb/ s OFDM signal transmission over 50m GI-POF. In OFC 2009, Yang reported 40Gb/ s signal transmission over 100m GI-POF based on discrete multimode modulation. By using the new spectral efficiency modulation format, such as CML and OFDM, can furthermore increase the bandwidth of the GI-POF.

Fiber model	50SR	62SR	120SR
Attenuation at 850nm	<60dB/ km		
Attenuation at 850nm	<60dB/ km		
Bandwidth at 850nm	>300MHz·km		
Numerical aperture	0.190±0.015	0.190±0.015	0.190±0.015
Macrobend loss	<0.25dB	<0.35dB	<0.60dB
Zero dispersion wavelength	1200~1650nm		
Dispersion slope	<0.06ps/ nm ² ·km		
Core diameter	50±5µm	62.5±/-5µm	120±/-10µm
Cladding diameter	490±/-5µm		
Temperature induced attenuation at 850nm (-20 to +70°C)	<5dB/ km		

Table 2. Specification of Thorlab's GI-POF.

In this section we will experimentally demonstrate the transmission of upconverted 16Gbit/ s OFDM signals on 24GHz microwave carrier over 50m GI-POF at 1310nm. The experimental setup of the proposed OFDM signals transmission over GI-POF is shown in Fig. 31. The lightwave from the DFB laser-diode (LD) at 1310nm with the output power around 10dBm is modulated by an intensity modulator (IM) driven by up-converted OFDM

signals. The 16Gbit/s OFDM signals are generated by OFDM transmitter and then up-converted to 24GHz to realize RF-OFDM signals via an electrical mixer. The up-converted spectrum is inserted in Fig. 29. We can see that the bandwidth of the OFDM signal is 8GHz. The OFDM baseband signal is generated offline and uploaded into a Tektronix AWG7102. The waveforms produced by the arbitrary wave generator (AWG) are continuously output at a sample rate of 20GHz (8bits DAC, 4GHz bandwidth). The FFT size is 256, from which 200 channels are used for data transmission, 55 channels at high frequencies are set to zero for over-sampling, and one channel in the middle of the OFDM spectrum is set to zero for DC in baseband. 10 training sequences are applied for each 150 OFDM-symbol frame in order to enable phase noise compensation. At the output of the AWG, the low-pass filter (LPF) with 5GHz bandwidth is used to remove the high-spectral components. Subsequently, the RF-pilot tone is created by inserting a small DC offset before an analogue I/Q mixer is used to up-convert the OFDM signal from the baseband to an 8.5GHz intermediate frequency (IF). The electrical spectrum of the original signal is shown in Fig. 32(a) that was measured at the point (a) in Fig. 31. The IM is driven by the OFDM signals to create double sideband (DSB) optical signals. The bias and the power of the RF signals are carefully adjusted to obtain proper power ratio between the optical carrier and the first-order sideband signals. After IM, the signal was launched into 50m of commercially available GI-POF for transmission. The core of the GI-POF is 50 μm with 60dB/km attenuation at 1300 nm. The signal power launched and output of GI-POF was 5.5 and 2.5dBm. A PIN receiver is used in the receiver side with the bandwidth of 29GHz and a 50 m multimode-coupled input. Before low pass filter (LPF), a 24GHz electrical LO signal is mixed to down-convert the electrical signal to its baseband form. The down-converted signals are sampled

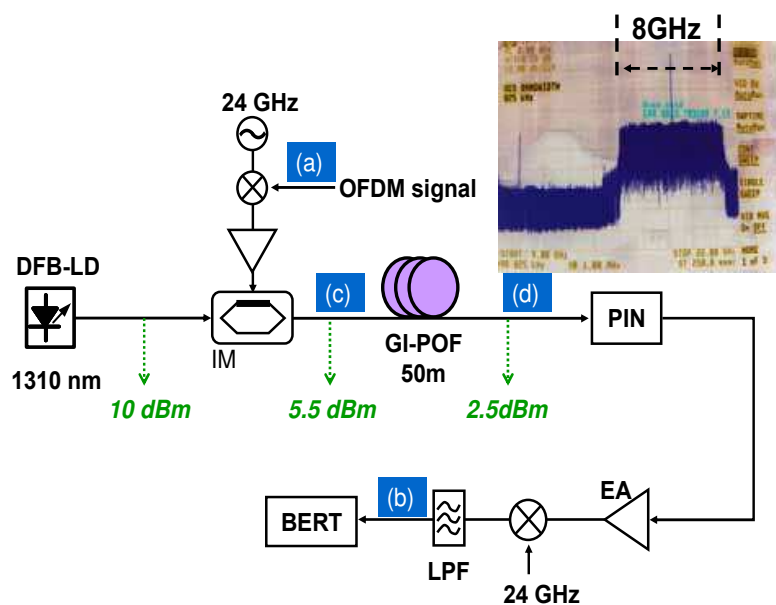


Fig. 31. Experimental configuration for 16Gb/s OFDM transmission over GI-POF. EA: electrical amplifier; IM: intensity modulator; GI-POF: graded-index plastic optical fiber; PIN: receiver; LPF: low pass filter. Inset: electrical spectrum of the OFDM signal after up-conversion.

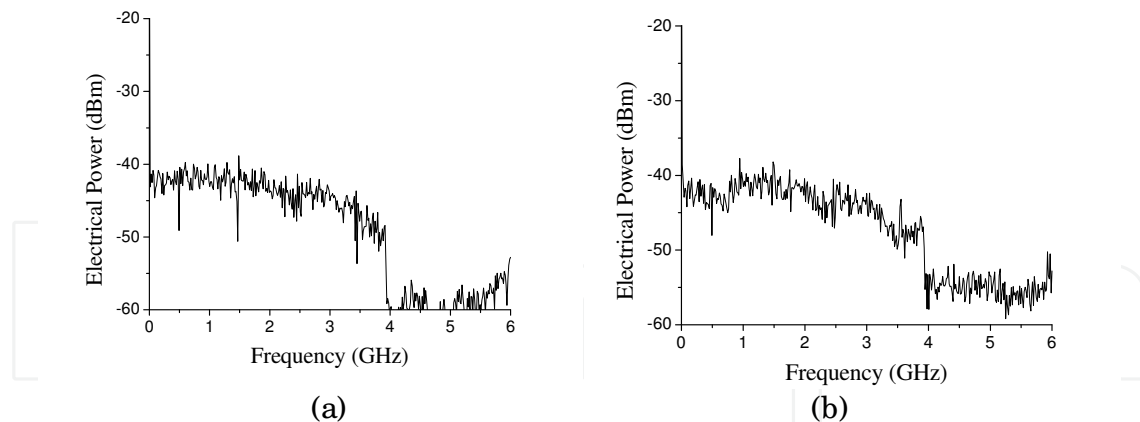


Fig. 32. Received electrical spectra: (a) after arbitrary waveform generator, (b) after LPF; received optical spectra with 0.01nm resolution.

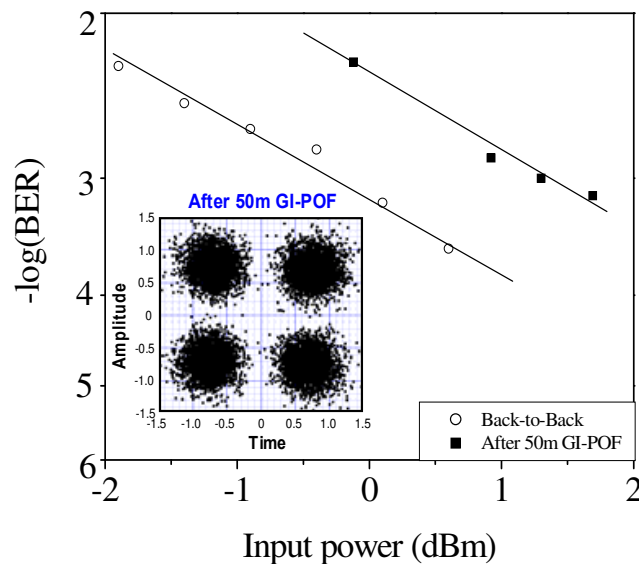


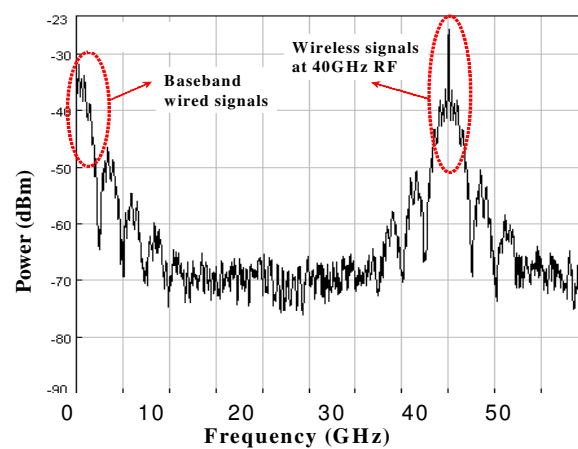
Fig. 33. Measured BER curves and the constellation figure of back-to-back and after 50m GI-POF.

with a real-time oscilloscope (Tektronix 6154C) and processed off-line. The electrical spectrum of down-converted signals is shown in Fig. 32(b). The measured BER of back-to-back and after transmission is shown in Fig. 33 and the constellation figure after 50m GI-POF is inserted. One million bits have been evaluated for all values of BER reported in this work. We can see that there exists signal degradation after 50m GI-POF. But the BER is still lower than 1×10^{-3} , which is below the limitation of forward error correction (FEC) at 2×10^{-3} . The main reason is the degradation of optical signal-to-noise-ratio (OSNR) from the fiber with an insertion loss of 3dB and modal dispersion.

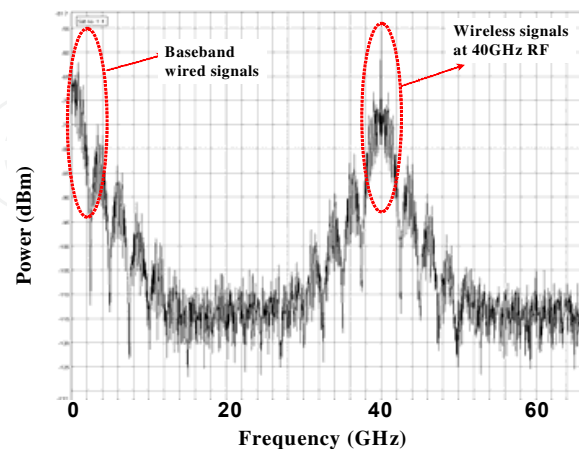
7. Testbed implementation for delivery of wired and wireless services simultaneously

Currently, the wired and wireless services are separately provided by two independent physical networks. Wired networks based on fiber-to-the-home (FTTH) access technologies

provide huge bandwidth to users but are not flexible enough to allow roaming connections. On the other hand, wireless networks offer mobility to users, but do not possess abundant bandwidth to meet the ultimate demand for video services with HDTV quality. Therefore, seamless integration of wired and wireless services for future-proof access networks will lead to convergence of ultimate high bandwidth for both fixed and mobile users in a single, low-cost transport platform. This can be accomplished by using our developed hybrid optical-wireless networks, which can not only transmit wireless signals at the BS over fiber, but also simultaneously provide the wired and wireless services to the end users due to the cascaded modulation scheme for downstream signals. Optical mm-waves can be generated by several all-optical up-conversion schemes that we have discussed in Section 2. No matter what kind of all-optical up-conversion scheme, one chooses, a part of base-band signal still exists in the whole electrical spectrum after all-optical up-conversion. To illustrate this point, we simulate the process of all-optical up-conversion schemes based on FWM in HNL-DSF and OCS modulation. As depicted in Fig. 34, it shows the electrical spectra after all-optical up-conversion. The LO frequency for all-optical up-conversion scheme based on FWM in fiber is 40 GHz and the baseband signal is 2.5-Gb/s NRZ signal. Fig.33 shows that there are



(a)



(b)

Fig. 34. Electrical spectra after all-optical up-conversion schemes. (a) FWM in HNL-DSF : LO signal is 40 GHz, (b) OCS modulation: RF driving frequency is 20 GHz.

two components of electrical signals after all-optical up-conversion, one part occupies the base-band, the other occupies high-frequency band near 40 GHz. Hence we propose a novel ROF network architecture to use the baseband signals for broadband optical access at 2.5 Gb/s at low cost and RF frequency for wireless connection.

Fig. 35 illustrates the architecture for concurrently providing super broadband wireless and wired services. The content providers or upstream networks send the data to the CO, where the multi-channel mm-wave carriers are generated through external modulator based on our developed all-optical up-converter. This up-conversion technique poses many advantages that allow data to be transmitted over wired and wireless medium in a single platform. First, the generation of the mm-wave carrier and the up-conversion of the original data channel are performed simultaneously in the optical domain. Second, as a result of this process, two identical data signals are generated concurrently: one at the electrical baseband and another at the RF-carrier frequency. The up-converted signals are multiplexed before they are transmitted over fiber to the BS where an AWG in WDM-PON is used to route the signals to customer premise. At the customer premise, the signal is divided by a PS into two. The first part is detected by a high-speed receiver and then electrically amplified using a narrow-band RF amplifier before broadcasted by an antenna as a wireless signal. The other part is sent directly to a wall-mounted optical port via fiber access, and a user can utilize a simple, low-cost receiver to detect the baseband data signal by filtering out the high frequency mm-wave signal. This newly hybrid system can allow wired and wireless transmission of the same content such as high-definition television, data and voice up to 100 times faster than current networks. The same services will be provided to customers who will either plug into the wired connection in the wall or access the same information through a wireless system. The customer premise can be conference centers, airports, hotels, shopping malls and ultimately homes and small offices.

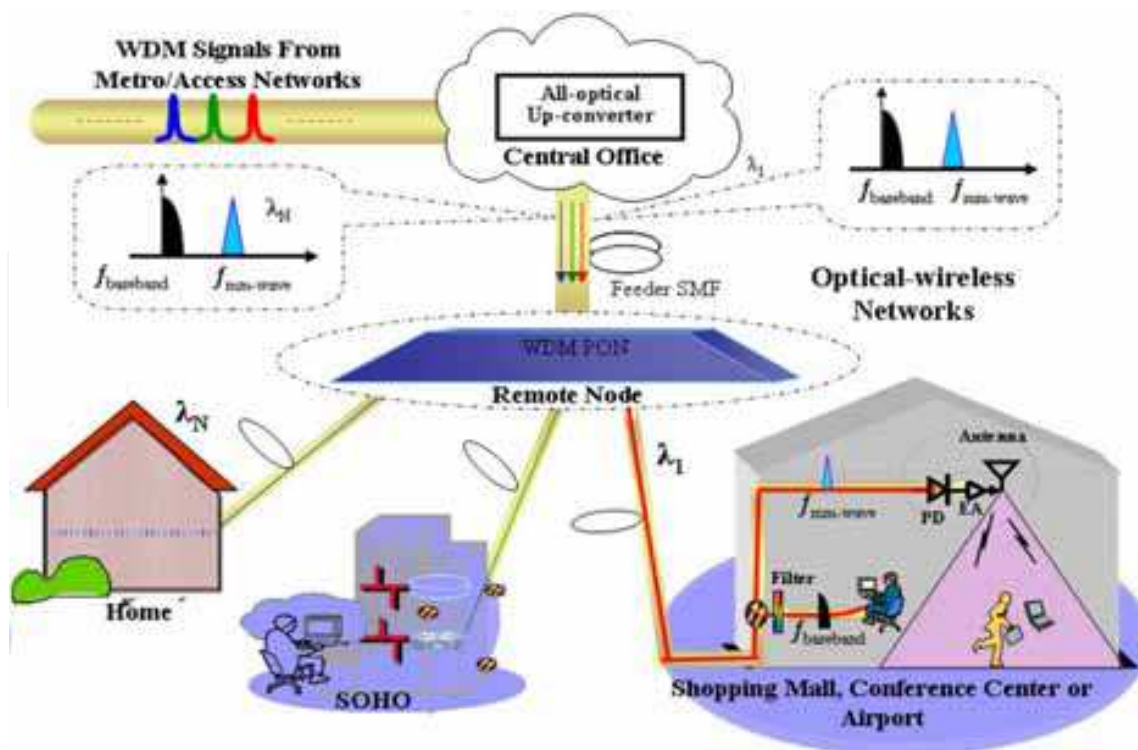


Fig. 35. Novel network architecture for providing dual-service in optical-wireless networks.

The experimental testbed setup for delivering wired and wireless services simultaneously is shown in Fig. 35. At the BS, the optical mm-wave is divided into two parts. The wired part is sent to a low-speed avalanche photodiode (APD) that has a 3-dB bandwidth of 2 GHz. Since the bandwidth of the APD receiver is limited at 2 GHz, the RF signal at high frequency is filtered out. In the case of the wireless part, the converted electrical signal is boosted by a RF electrical amplifier before it is broadcasted through a double ridge guide antenna with a gain of 19.2 dBi at frequency range of 18 to 40 GHz. After wireless transmission, the signal is received by another identical mm-wave antenna. The signal is down-converted through a mixer and TD line by using part of the incoming signal as the LO signal. The receiver sensitivities and eye diagrams at different air distances are shown in Fig. 37. The power

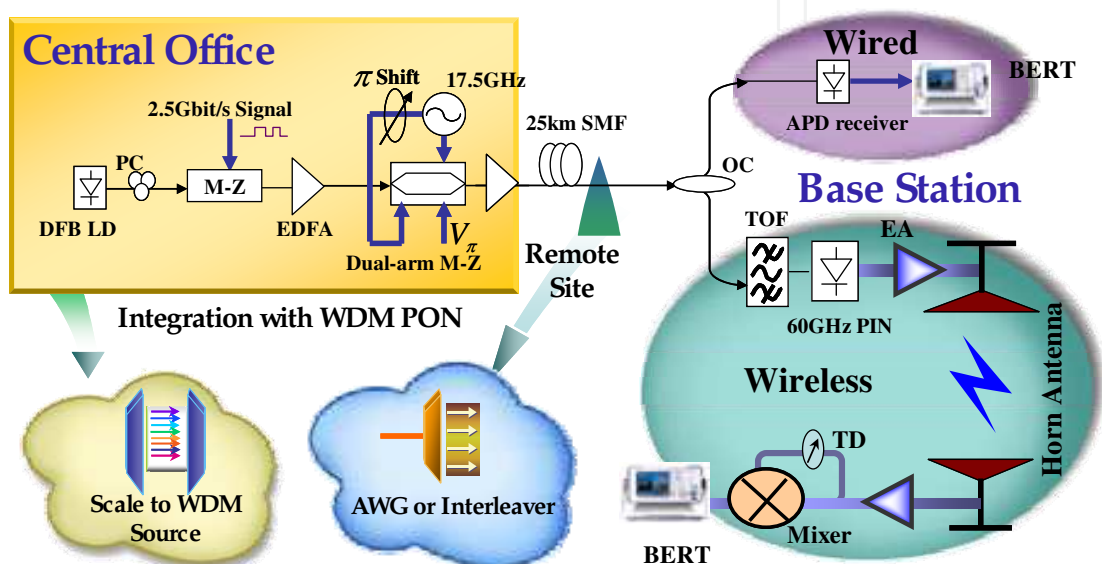


Fig. 36. Testbed setup for delivering wired and wireless services simultaneously.

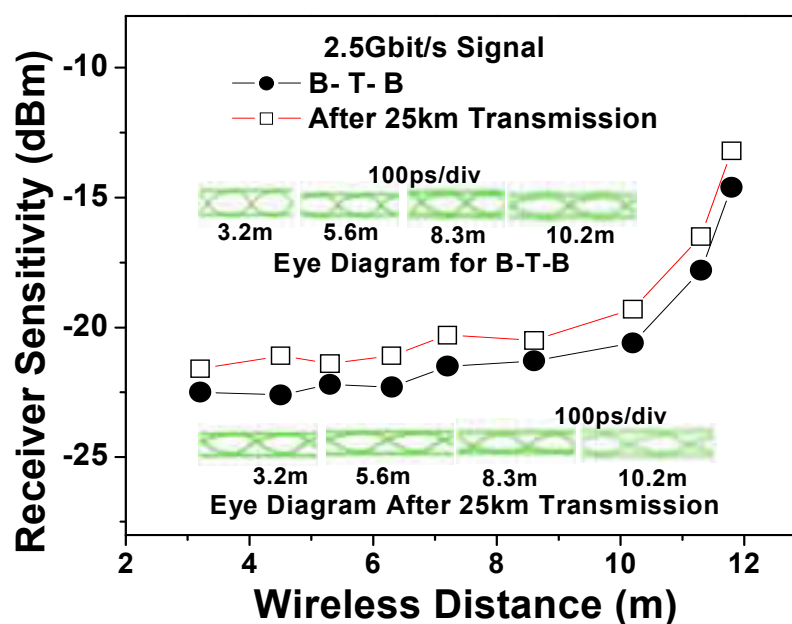


Fig. 37. Receiver Sensitivity for 2.5-Gb/s signal at different air distance.

penalty after transmission over 25-km SMF is less than 1.5 dB. The receiver sensitivity degrades quickly when the wireless signals are transmitted beyond 10-m indoor air space because the antenna as an isotropic point source in its radiation direction spreads its energy over a certain angle of surface area as the wave propagates in air space. The path loss is proportional to the reciprocal of distance square. Signal degradation via multiple reflections from the wall is a key factor that limits the maximum transmission distance for 2.5-Gb/s wireless signal in our testbed environment of office building hallway.

Fig. 38 shows the system implementation of the first field demonstration of delivering dual service uncompressed 270-Mbps standard definition (SD) and uncompressed 1.485-Gbps high definition (HD) video content using 2.4-GHz microwave and 60-GHz mm-wave radio signals, respectively, over Georgia Institute of Technology (GT) Campus fiber backbone network from *Centergy Research Lab* at 10th Street to *Aware Home Residential Lab* at 5th Street. The transmission distance is 2.5 km standard single-mode fiber (SMF-28). At the transmitter (*Centergy building*), all optical up-conversion method is used to perform simultaneous generation of 60-GHz mm-wave and up-conversion of 1.485-Gbps HD signals at wavelength 1554.0 nm. The all-optical mm-wave generation at 60-GHz is realized by using an optical phase modulator driven by 30-GHz sinusoidal electrical clock signal and an optical de-interleaver as described in the previous section. The HD signal at 1.485-Gbps is generated from the component output of commercially available Sony Blue-Ray Disc player and an analog-to-digital converter. For 2.4-GHz radio signal, we used electrical mixing and double-sideband optical modulation to up-convert 270-Mbps real-time SD video content generated from a commercially available Canon Camcorder before optically transmitted at wavelength of 1550 nm. At the receiver (*Aware home*), direct detection of optical 60-GHz mm-wave signal is performed by a 60-GHz bandwidth PIN photodiode to realize optical-to-electrical

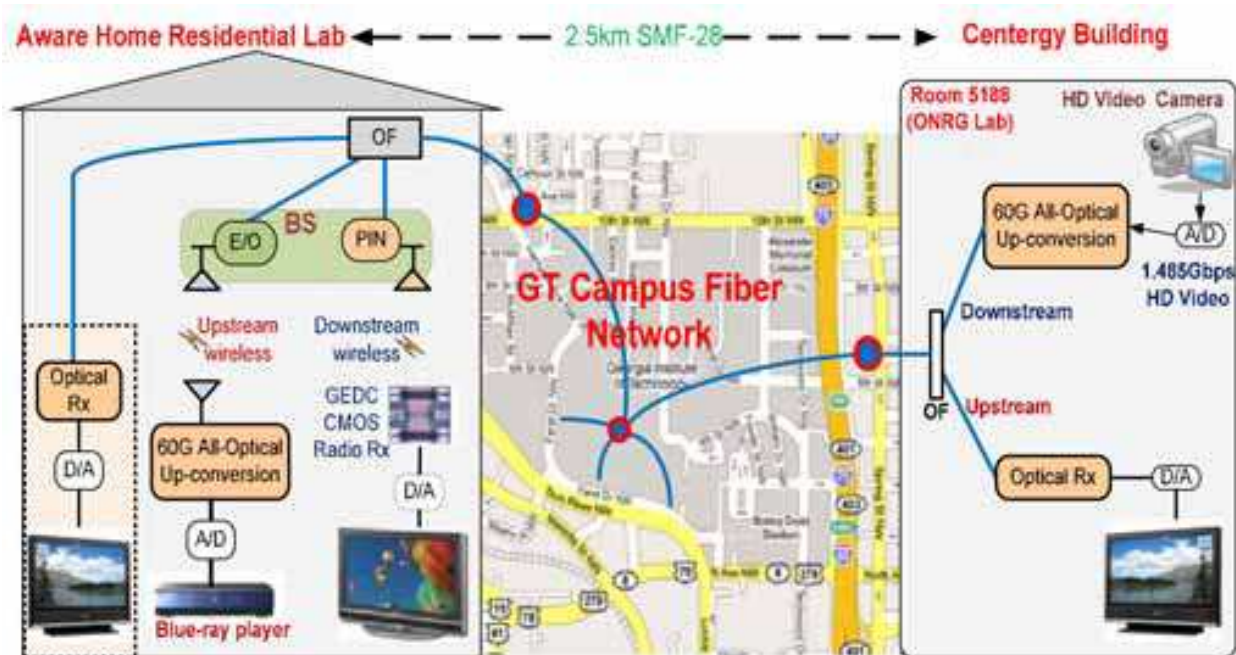


Fig. 38. Field trial demonstration setup of the SD/ HD video content delivery using 2.4-GHz and 60-GHz mm-wave radio-over-fiber in the Georgia Tech (GT) campus fiber network.

conversion. The converted electrical mm-wave signal is then amplified by an electrical amplifier (EA) with 5 GHz bandwidth centered at 60 GHz and 3.55 before it is broadcasted through a double-ridge guide rectangular horn antenna with a gain of 25 dBi, frequency range of 50 to 75 GHz and 3 dB beam width of 7°. After the wireless transmission, the 60-GHz mm-wave signal is received by the end mobile terminal in order to perform the down-conversion and recover the 1.485-Gbps HD video signal. The down-conversion is performed by a 60-GHz balanced mixer using self-reflective mixing technique. Similarly, the 2.4-GHz radio signal is received by a 2.5-GHz PIN receiver at the BS and distributed over the wireless to the receiver antenna. The 270-Mbps SD signal is then recovered by down-conversion process. Fig. 39 shows the transmitter and receiver modules at two separate locations. We did not measure any BER in the field-trial, since we do not have any available electrical clock recovery module that is required to recover the clock at the distantly located receiver. However, the video quality displayed at the remote receiver TV screens located at



Fig. 39. Transmitter and receiver of the 3-screen, dual-service 2.4-GHz and 60-GHz RoF carrying 270-Mbps SD and 1.485-Gbps HD video content. (a) Transmitter at Centergy lab at 10th Street, (b) 60-GHz Wireless setup at residential lab at 5th Street, and (c) 3-screen receiver at residential lab.

the residential lab (2.5 km away from the transmitter at Centergy building) indicates the very good BER performance of the received signal.

ROF-based optical-wireless access networks have been considered the most promising solution to increase the capacity, coverage, bandwidth, and mobility as well as decreasing cost for next-generation access networks. This hybrid system explore the converged benefits of the optical and wireless technology to serve both fixed and mobile end users. However, there are many issues that still need to be addressed. The media access control (MAC) is a promising direction for future research. Although the analog nature of ROF links offers transparency for the transmission of the wireless protocol stack, the additional propagation delay introduced by the fiber in the end-to-end logical link connection limits the maximum fiber lengths that can be accommodated to guarantee sufficiently low latency for adequate protocol performance. Another research area would be the FDM design for optical-wireless systems. OFDM is a good choice for wireless transmission, but the OFDM-ROF system has the stringent requirement of orthogonality between the sub-carriers. Since there are 7-GHz license-free spectrum, the traditional FDM can be used in the optical-wireless system to reduce the complexity of signal processing and increase the tolerance towards the frequency drift.

8. Acknowledgment

Author likes to thank Dr. T. Wang from NEC Laboratories America and Dr. M. Huang and Dr. A. Chowdhury from Georgia Institute of Technology for their great contribution for these studies.

9. References

- M. Huchard, M. Weiss, A. Pizzinat, S. Meyer, P. Guignard, and B. Charbonnier (2008). Ultra-Broadband wireless home network based on 60-GHz WPAN cells interconnected via RoF, *J. of Lightwave Technol.*, 26(15), 2364-2372.
- C. T. Lin, W. R. Peng, P. C. Peng, J. Chen, C. F. Peng, B. S. Chiou, and S. Chi (2006). Simultaneous Generation of Baseband and Radio Signals Using Only One Single-Electrode Mach-Zehnder Modulator With Enhanced Linearity, *IEEE Photon. Technol. Lett.*, 18, 2481-2483.
- N. J. Gomes, A. Nkansah, and D. Wake (2008), Radio-Over-MMF techniques—part I: RF to microwave frequency systems, *J. of Lightwave Technol.*, 26(15), 2388-2395.
- A. M. J. Koonen, and M. G. Larrodé (2008). Radio-Over-MMF techniques—part II: microwave to millimeter-wave systems, *J. of Lightwave Technol.*, 26(15), 2396-2408.
- L. Chen, H. Wen and S. C. Wen (2006). A radio-over-fiber system with a novel scheme for millimeter-wave generation and wavelength reuse for up-link connection, *IEEE Photon. Technol. Lett.*, 18, 2056-2058.
- A. Stöhr, A. Akrouf, R. Buß, B. Charbonnier, F. v. Dijk, A. Enard, S. Fedderwitz, D. Jäger, M. Huchard, F. Lecoche, J. Marti, R. Sambaraju, A. Steffan, A. Umbach, and M. Weiß (2009). 60 GHz radio-over-fiber technologies for broadband wireless services, *J. of Optical Networking*, 8(5), 471-487.
- J. Yu, et al. (2007). A cost-effective scheme to generate and de-multiplex multiple frequency millimeter-wave signals in a ROF network, *ECOC 2007*, 3.3.3.

- J. Ma, J. Yu, C. Yu, X. Xin, Q. Zhang (2007). Transmission performance of the optical mm-wave generated by double sideband intensity-modulation, *Optics Communications*, 280(2), 317-326.
- J. Ma, J. Yu, C. Yu, X. Xin (2007). Fiber dispersion influence on transmission of the optical millimeter-wave generated by LN-MZM intensity modulation, *IEEE/OSA Journal of Light. Technol.*, 25(11).
- C. Bock, J. Prat, S. D. Walker (2005). Hybrid WDM/ TDM PON using the AWG FSR and featuring centralized light generation and dynamic bandwidth allocation, *J. Lightw. Technol.*, 23(12), 3981-3988.
- S.-J. Park, C.-H. Lee, K.-T. Jeong, H.-J. Park, J.-G. Ahn, K.-H. Song (2004). Fiber-to-the-home services based on wavelength-division-multiplexing passive optical network, *J. Lightw. Technol.*, 22(11), 2582-2591.
- H. Bolcskei, A. J. Paulraj, K.V.S. Hari, R. U. Nabar, W. W. Lu (2001). Fixed broadband wireless access: state-of-the-art, challenges, and future directions, *IEEE Commun. Mag.*, 100-108.
- B. Fong, N. Ansari, A. C. M. Fong, G. Y. Hong, P. B. Rapajic (2004). On the scalability of fixed broadband wireless access network deployment, *IEEE Commun. Mag.*, 42(9), S12-S18.
- S. J. Vaughan-Nichols (2004). Achieving wireless broadband with WiMax, *Computer*, 37(6), 10-13.
- A. Chowdhury, H. Chien, M. Huang, J. Yu and G. K. Chang (2008). Rayleigh Backscattering Noise-Eliminated 115-km Long-Reach Bidirectional Centralized WDM-PON With 10-Gb/ s DPSK Downstream and Remodulated 2.5-Gb/ s OCS-SCM Upstream Signal, *IEEE Photon. Technol. Lett.*, 20(24), 2081-2083.
- J. Yu, Z. Jia, T. Wang, G. K. Chang (2007). Centralized Lightwave Radio-Over-Fiber System With Photonic Frequency Quadrupling for High-Frequency Millimeter-Wave Generation, *IEEE Photon. Technol. Lett.*, 19(19), 1499 – 1501.
- J. Yu et al (2007). Demonstration of a Novel WDM Passive Optical Network Architecture to Provide Triple Play Services with Source-free Optical Network Units, *IEEE Photon. Technol. Lett.*, 19(8), 571-573.
- Z. Jia, J. Yu, A. Chowdhury, G. Ellinas, G. K. Chang (2007). Simultaneous Generation of Independent Wired and Wireless Services Using a Single Modulator in Millimeter-Wave-Band Radio-Over-Fiber Systems, *IEEE Photon. Technol. Lett.*, 19(20), 1691 – 1693.
- J. Yu, M. Huang, Z. Jia, A. Chowdhury, G.-K. Chang (2009). All-Optical Up-Conversion for 30x7.5Gb/ s WDM Signals in a 60GHz ROF System, *OFC 2009*, OTuB4.
- H.-C. Chien, A. Chowdhury, Y.-T. Hsueh, Z. Jia, S.-H. Fan, J. Yu, G.-K. Chang (2009). A Novel 60-GHz Millimeter-Wave over Fiber with Independent 10-Gbps Wired and Wireless Services on a Single Wavelength Using PolMUX and Wavelength-Reuse Techniques, *OFC 2009*, OTuB7.
- Y.-T. Hsueh, Z. Jia, H.-C. Chien, A. Chowdhury, J. Yu, G.-K. Chang (2009). Generation and Transport of Independent 2.4 GHz (Wi-Fi), 5.8 GHz (WiMAX), and 60-GHz Optical Millimeter-Wave Signals on a Single Wavelength for Converged Wireless over Fiber Access Networks, *OFC 2009*, OTuJ1.

- D. Qian, N. Cvijetic, Y.-K. Huang, J. Yu, T. Wang (2009). 22.4-Gb/s OFDM Transmission over 1000 km SSMF Using Polarization Multiplexing with Direct Detection, *OFC 2009*, OTuO7.
- Z. Ja, H.-C. Chien, Y.-T. Hsueh, A. Chowdhury, J. Yu, G.-K. Chang (2009). Wireless HD Services over Optical Access Systems: Transmission, Networking, and Demonstration, *OFC 2009*, JThA84.
- J. Ma, J. Yu, C. Yu, Z. Ja, G.-K. Chang (2007). The influence of fiber dispersion on the code form of the optical mm-wave signals generated by single sideband intensity-modulation, *Optics Communications*, 271(2), 396-403.
- D. Wake, M. Webster, G. Wimpenny, K. Beacham, L. Crawford (2004). Radio over fiber for mobile communications, in *Int. Topical Meeting Microwave Photonics*, 157-160.
- K. Kitayama (2000). Architectural considerations of fiber radio millimeter wave wireless access systems," *Fiber Integr. Opt.* 19, 167-186.
- L. Rosa, S. Selleri, G. Tartarini, P. Faccin, E.M. Fabbri (2006). Distortion Performance Prediction in Multi-Band Radio over Fiber Systems Exploiting Direct Laser Modulation, *36th European Microwave Conference*, 1292-1295.
- K.E. Razavi, P.A. Davies (1997). Millimetre wave generation by filtering the FM-IM spectra of a directly modulated DFB laser, *IEEE MTT-S Int. Microw. Symposium Digest*, 3, 1707-1708.
- L. A. Johansson, A. J. Seeds (2000). Millimetre-wave radio-over-fibre transmission using an optical injection phase-lock loop source, *Microwave Photonics*, 129-132.
- B. Leesti, A. J. Zilkie, J. S. Aitchison, M. Mojahedi, R. H. Wang, T. J. Rotter, C. Yang, A. Stintz, and K. J. Malloy (2005). Broad-band wavelength up-conversion of picosecond pulses via four-wave mixing in a quantum-dash waveguide, *IEEE Photon. Technol. Lett.*, 17(5), 1046-1048.
- J.-H. Seo, Y.-K. Seo, and W.-Y. Choi (2003). Nonlinear characteristics of an SOA photonic frequency up-converter, *Int. Topical Meeting on Microwave Photonics*, 109-112.
- H.-J. Song, J.-S. Lee and J.-I. Song (2004). Signal up-conversion by using a cross-phase-modulation in all-Optical SOA-MZI wavelength converter", *IEEE Photon. Technol. Lett.*, 16(2), 593-595.
- J. Ma, J. Yu, C. Yu, Z. Ja, X. Sang, Z. Zhou, T. Wang, G.K. Chang (2006). Wavelength conversion based on four-wave mixing in high-nonlinear dispersion shifted fiber using a dual-pump configuration, *J. Lightw. Technol.*, 24(7), 2851-2858.
- J. Yu, J. Gu, X. Liu, Z. Ja and G. K. Chang (2005). Seamless integration of an 8x 2.5Gb/s WDM-PON and Radio-Over-Fiber using all-optical up-conversion based on Raman-assisted FWM, *IEEE Photon. Technol. Lett*, 17(9), 1986-1988.
- W. Wang, H. N. Poulsen, L. Rau, D. J. Blumenthal (2003), Regenerative 80-Gb/s fiber XPM wavelength converter using a hybrid Raman/ EDFA gain-enhanced configuration, *IEEE Photon. Technol. Lett*, 15(10), 1416-1418.
- J. Yu, X. Zheng, C. Peucheret, A. T. Clausen, H. N. Poulsen, and P. Jeppesen (2000), All-optical wavelength conversion of short pulses and NRZ signals based on a nonlinear optical loop mirror, *J. Lightw. Technol.*, 18(7), 1007-1017.
- W. Wang, H. N. Poulsen, L. Rau, H.-F. Chou, J. E. Bowers, D. J. Blumenthal (2005). Raman-enhanced regenerative ultrafast all-optical fiber XPM wavelength converter, *J. Lightw. Technol.*, 23(3), 1105-1115.

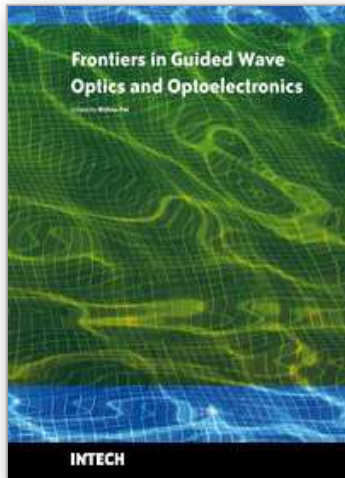
- Z. Jia, J Yu, G.-K. Chang (2005). All-optical 16x2.5 Gbit/ s WDM signals simultaneous up-conversion based on XPM in an NOLM in ROF systems, *IEEE Photon. Technol. Lett.*, 17(12), 2724-2726.
- C. Lim, M. Attygalle, A. Nirmalathas, D. Novak, R. Waterhouse (2006). Analysis of optical carrier-to-sideband ratio for improving transmission performance in fiber-radio links, *IEEE Trans. on Microw. Theory and Tech.*, 54(5), 2181-2187.
- P. S. Cho, D. Mahgerefteh, and J. Goldhar (1999). All-Optical 2R Regeneration and Wavelength Conversion at 20 Gb/ s Using an Electroabsorption Modulator, *IEEE Photon. Technol. Lett.*, 11(12), 1662 –1664.
- J Yu, Z. Jia, T. Wang, and G. K. Chang (2007). A novel radio-over-fiber configuration using optical phase modulator to generate an optical mm-wave and centralized lightwave for uplink connection, *IEEE Photon. Technol. Lett.*, 19, 140–142.
- W. Shieh, X. Yi, Y. Tang (2007). Experimental Demonstration of Transmission of Coherent Optical OFDM Systems, *OFC 2007, OMP2*.
- A. M. Odlyzko (2003). Internet traffic growth: Sources and implications,” in *Proc. SPIE: Optical Transmission systems and Equipment WDM Networking II*, 5427, 1-15.
- J Halpern and G. Garceau (2004). *Fiber: Revolutinizing the Bell's Telecome Networks*. New York: Bernstein/ Telcordia Technologies Study.
- B. Bing (2006). Broadband wireless access – the next wireless revolution, *Proceedings of the 4th Annual Communication Networks and Services Research Conference*, pp. 14.
- D. Chrissan (2004). Uni-DSL: One DSL for universal service, *Texas Instruments White Paper (Spay018)*.
- C. Lee, W. V. Sorin, B. Y. Kim (2006). Fiber to the home using a PON infrastructure, *J. Lightw. Technol.*, 24(12), 4568-4582.
- T. Koonen (2006). Fiber to the home/ fiber to the premises: what, where and when? *Proc. of the IEEE*, 94(5), 911-934.
- J Yu, D. Qian, M. Huang, Z. Jia, G. K. Chang, T. Wang (2008). 16Gbit/ s radio OFDM signals over graded-index plastic optical fiber, *ECOC 2008*, P. 6. 16.
- D. Qian, J Yu, J Hu, L. Zong, L. Xu, T. Wang (2008). 8x11.5Gbit/ s OFDM transmiión over 1000km SSMF using convencional DFB lasers and direct-detection, *OFC 2008, OMM3*.
- J Yu, J Hu, D. Qian, Z. Jia, G. K. Chang, T. Wang (2008). Transmission of micro-wave photonics generated 16Gbit/ s super broadband OFDM signals in radio-over-fiber system, *OFC 2008, OThP2*.
- M. Huang, J Yu, H. Chien, A. Chowdhury, J Chen, S. Chi, G. K. Chang (2008). A simple WDM-PON architecture to simultaneously provide triple-play services by suing one single modulator, *OFC 2008, OTuI4*.
- Z. Jia, J Yu, D. Qian, G. Ellinas, G. K. Chang (2008). Experimental demonstration for delivering 1Gbit/ s OFDM signals over 80-km SSMF in 40GHz Radio-over-fiber access systems, *OFC 2008, JWA108*.
- Z. Jia, J Yu, L. Zong, G. K. Chang (2008). Transport of 8x2.5Gbit/ s gíreles signals over optical millimeter wave through 12 straight-line WSSs and 160km fiber for advanced DWDM metro ntworks, *OFC 2008, OMO3*.
- K. I. Kitayama and R. A. Griffin (1999). Optical downconversion from millimeter-wave to IF-Band over 50km long optical fiber link using an electroabsorption modulator, *IEEE Photon. Technol. Lett.*, 11(2), 287-289.

- K. Nishimura, R. Inohara, M. Usami, S. Akiba (2005). All-optical wavelength conversion by electroabsorption modulator, *IEEE J. Sel. Topics in Quantum Electronics*, 11(1), 278 – 284.
- J. Yu, Z. Jia, G.-K. Chang (2005). All-optical mixer based on cross-absorption modulation in electroabsorption modulator," *IEEE Photon. Technol. Lett.*, 17(11), 2421-2423.
- D. Wake, C. R. Lima, P. A. Davies (1996). Transmission of 60GHz signals over 100km of optical fiber using a dual-mode semiconductor laser," *IEEE Photon. Technol. Lett.*, 8(4), 578-580.
- U. Gliese, S. Norskov, T. N. Nielsen (1996). Chromatic dispersion in fiber-optic microwave and millimeter-wave links," *IEEE Trans. Microw. Theory and Tech.*, 44(10), 1716-1724.
- G. Qi, J. Yao (2005). Optical generation and distribution of continuously tunable millimeter-wave signals using an optical phase modulator, *J. Lightw. Technol.*, 23(9), 2687-2695.
- J. Yu, Z. Jia, L. Xu, L. Chen, T. Wang, G.-K. Chang (2006). DWDM optical millimeter-wave generation for radio-over-fiber using an optical phase modulator and an optical interleaver, *IEEE Photon. Technol. Lett.*, 18(13), 1418-1420.
- M.G. Larrode, A. M. J. Koonen, J. J. V. Olmos, A. Ng'Oma (2006). Bidirectional radio-over-fiber link employing optical frequency multiplication," *IEEE Photon. Technol. Lett.*, 18(1), 265–267.
- J.-H. Seo, C.-S. Choi, Y.-S. Kang, Y.-D. Chung, J. Kim, W.-Y. Choi (2006). SOA-EAM frequency up/ down-converters for 60-GHz bi-directional radio-on-fiber systems, *IEEE Trans. Microw. Theory Tech.*, 54(2), 959-966.
- P. J. Winzer, R.-J. Essiambre (2006). Advanced optical modulation format, *Proc. Of the IEEE*, 94(5), 952-985.
- W. Huang, C.-K. Chan, L.-K. Chen, and F. Tong (2005). An optical network unit for WDM access networks with downstream DPSK and upstream remodulated OOK data using injection-locked FP laser, *IEEE Photon. Technol. Lett.*, vol. 15, no. 10, pp. 1476–1478, Oct. 2005.
- Z. Jia, J. Yu, M. Haris, D. Boivin, G.-K. Chang (2006). A bi-directional radio-over-fiber system with all-optical up-converted DPSK for downstream and re-modulated OOK for upstream, *Proc. LEOS 2006, TuV3*.
- J. J. V. Olmos, T. Kuri, and K.-I. Kitayama (2009). Half-duplex 12-channel dense WDM 2.6-GHz-band radio-over-fiber system employing a 1.5 GHz bandwidth reflective semiconductor optical amplifier, *J. of Optical Networking*, 7(12), 989-994.
- I. G. Insua, D. Plettemeier, and C. G. Schäffer (2009). Broadband radio-over-fiber-based wireless access with 10 Gbits/s data rates, *J. of Optical Networking*, 8(1), 77-83.
- Z. Jia, J. Yu, G.-K. Chang (2006). A full-duplex radio-over-fiber system based on optical carrier suppression and reuse, *IEEE Photon. Technol. Lett.*, 18(16), 1726–1728.
- H. Shinohara (2005). Broadband access in Japan: rapidly growing FTTH market, *IEEE Commun. Mag.*, 43(9), 72-78.
- G.-K. Chang, J. Yu, Z. Jia, J. Yu (2006). Novel optical-wireless access network architecture for simultaneously providing broadband wireless and wired services, *Proc. OFC 2006, Anaheim, CA, OFM1*.
- Z. Xu, Y. Wen, M. Attygalle, X. Cheng, and W. Zhong (2006). Multiple channel carrier-reused WDM passive optical networks, *ECOC 2006, Th 4.3.2*.
- M. Attygalle et al., (2006). Wavelength reuse scheme for source free optical network units in WDM passive optical networks, *ECOC 2006, Th 3.5.3*.

- W.Hung, C. K. Chan, L. K. Chen, and F. Tong (2003). An optical network unit for WDM access networks with downstream DPSK and upstream remodulated OOK data using injection-lock FP laser, *IEEE Photon. Technol. Lett.*, 15(10), 1476-1478.
- E. Wong, K.L. Lee, T.Anderson (2006). Directly Modulated Self-Seeding Reflective SOAs as Colorless Transmitters for WDM Passive Optical Networks, *OFC 2006*, PDP 49.
- O. Akanbi et al (2005). A new bidirectional DWDM PON using optical carrier suppression and separation in the central office, *ECOC 2005*, We. 3. 3. 1.
- M. Khanal, C. J Chae, and R. S. Tucker (2005). Selective broadcasting of digital video signals over a WDM passive optical network”, *IEEE Photon. Technol. Lett.*, 17(9), 1992-1994.
- J Yu, O. Akanbi, Y. Luo, L. Zong, Z. Jia, T. Wang and G. K. Chang (2007). A novel WDM-PON architecture with centralized lightwaves in OLT for providing triple play services, *OFC 2007*.
- M. Attygalle, C. Lim, G. J Pendock, A. Nirmalathas, and G. Edvell (2005). Transmission improvement in fiber wireless links using fiber Bragg gratings, *IEEE Photon. Technol. Lett.*, 17(1), 190-192.
- A. Wiberg, P. Perez-Millan, M. V. Andres, P. A. Andrekson, P. O. Hedekvist (2005). Fiber-optic 40-GHz mm-wave link with 2.5Gb/ s data transmission, *IEEE Photon. Technol. Lett.*, 17(9), 1938-1940.
- G. H. Smith, D. Novak, Z. Ahmed (1997). Overcome chromatic-dispersion effects in fiber-wireless systems incorporating external modulators, *IEEE Trans. on Microw. Theory and Tech.*, 45(8), 1410-1415.
- J. M. Fuster, J. Marti, J. L. Corral, V. Polo, F. Ramos (2000). Generalized study of dispersion-induced power penalty mitigation techniques in millimeter-wave fiber-optic links, *J. of Lightw. Technol.* 18(7), 933-940.
- C. K. Sun, R. J Orazi, S. A. Pappert (1996). Efficient microwave frequency conversion using photonic link signal mixing,” *IEEE Photon. Technol. Lett.*, 8(1), 154-156.
- J Yu, Z. Jia, L. Yi, Y. Su, G.-K. Chang, T. Wang (2006). Optical millimeter-wave generation or up-conversion using external modulators, *IEEE Photon. Technol. Lett.*, 18(1), 2006.
- J Yu, Z. Jia, T. Wang, G. K. Chang and G. Ellinas (2007). Demonstration of a novel WDM-PON access network compatible with ROF system to provide 2.5Gb/ s per channel symmetric data services, *OFC 2007*.
- J. E. Mitchell (2004). Performance of OFDM at 5.8 GHz using radio over fiber link, *Electronics Letters*, 40(21), 1353- 1354.
- W. Shieh, X. Yi, and Y. Tang (2007). Transmission experiment of multi-gigabit coherent optical OFDM systems over 1000km SSMF fiber, *Electron. Lett.*, 43, 183-184.
- H. Bao (2007). Transmission simulation of coherent optical OFDM signals in WDM systems, *Optics Express*, 15, 4410-4418.
- Y. Tang, W. Shieh, X. Yi, and R. Evans (2007). Optimum design for RF-to-optical up-converter in coherent optical OFDM systems, *IEEE Photon. Technol. Lett.* 19, 483-485.
- A. Kim, Y. H. Jo, and Y. Kim (2004). 60GHz wireless communication systems with radio-over-fiber links for indoor wireless LANs, *IEEE Transactions on Consumer Electronics*, 50, 517-520.
- L. Chen, J He, Y. Li. (2007). Simple ROF configuration to simultaneously realize optical millimeter-wave signal generation and source-free base station operation, *ECOC 2007*, 45-46.

- T. Kawanishi, K. Higuma, T. Fujita, S. Mori, S. Oikawa, J. Ichikawa, T. Sakamoto, and M. Izutsu (2005). 40 Gbit/s versatile LiNbO lightwave modulator, *ECOC 2005*, Glasgow, Scotland, 2005, Th 2.2.5.
- Z. Jia, J. Yu, Y.-T. Hsueh, H.-C. Chien, G.-K. Chang (2008). Demonstration of a symmetric bidirectional 60-GHz radio-over-fiber transport system at 2.5-Gb/s over a single 25-km SMF-28, *ECOC 2008*, Tu. 3. F. 5.
- D. Qian, J. Yu, J. Hu, P. N. J., T. Wang (2008). 11.5-Gb/s OFDM transmission over 640km SSMF using directly modulated laser, *ECOC 2008*, Mo. 3. E. 4.
- M.-F. Huang, J. Yu, Q. Dayou, G.-K. Chang (2008). Lightwave centralized WDM-OFDM-PON, *ECOC 2008*, Th. 1.F.5.
- T. Sakamoto, T. Kawanishi, and M. Izutsu (2006). Continuous-phase frequency-shift keying with external modulation, *IEEE J. Sel. Topics Quantum Electron.*, 12(4), 589–595.
- J. Yu et al. (2005). A novel optical frontend for ultra-high capacity of 32x2.5Gbit/s data delivery in radio-over-fiber systems, *ECOC 2005*, Th 4.5.4.
- M. Attygalle et al. (2006). Wavelength reuse scheme for source free optical network units in WDM passive optical networks, *ECOC 2006*, Th 3.5.3.
- M. R. Wiech et al. (2006). Bidirectional EDFA for future extra large passive optical networks, *ECOC 2006*, Mo. 4. 5. 7.
- Z. Xu, X. Zhang and J. Yu (2007). Frequency up-conversion of multiple RF signals using optical carrier suppression for radio over fiber downlinks, *Optics Express*, 15(25), 16737-16747.
- K. Kitayama, R. Griffin (1999). Optical downconversion from millimeter-wave to IF band over 50-km-long optical fiber link using an electroabsorption modulator, *IEEE Photon. Technol. Lett.*, 11, 287-289.
- J. Ma, J. Yu, Z. Jia, C. Yu, Z. Zhou, and G.-K. Chang (2007). Optical mm-wave generation based on phase modulation along with optical filtering, *Microwave and Optical Technol. Lett.*, 49(8), 1787-1793.
- S.L. Jansen, et al (2007). 20-Gb/s OFDM Transmission over 4,160-km SSMF Enabled by RF-Pilot Tone Phase Noise Compensation, in proc. *OFC 2007*, PDP 15.
- S. Jansen, I. Morita, H. Tanaka (2007). 10-Gb/s OFDM with conventional DFB lasers, *ECOC 2007*, 5.2.2.
- L. Xu, J. Hu, D. Qian and T. Wang (2008). Coherent optical OFDM systems using self optical carrier extraction, *OFC 2008*, OMu4.
- G. K. Chang, Z. Jia, J. Yu (2006). Super-broadband optical wireless over optical fiber network architecture, *LEOS 2006*, TuV1.
- J. Yu, Z. Jia, T. Wang, G.-K. Chang and G. Ellinas (2007). Demonstration of a novel WDM-PON access network compatible with ROF systems to provide 2.5Gb/s per channel symmetric data services, *OFC 2007*, OThM5.
- J. Yu, Z. Jia and G.-K. Chang (2005). Seamless integration and large coverage delivery of 32x2.5Gbit/s DWDM signals in a radio-over-fiber network, *ECOC 2005*, Th4.5.4.
- J. Ma, X. Xin, J. Yu, C. Yu, K. Wang, H. Huang, and L. Rao (2009). Optical millimeter wave generated by octupling the frequency of the local oscillator, *J. of Optical Networking*, 7(10), 837-845.
- J. Chen, C.-T. Lin, P. T. Shih, W.-J. Jang, S.-P. Dai, Y.-M. Lin, P.-C. Peng, and S. Chi (2009). Generation of optical millimeter-wave signals and vector formats using an integrated optical I/Q modulator, *J. of Optical Networking*, 8(2), 188-200.

- C. Lim, A. Nirmalathas, M. Bakaul, K.-L. Lee, D. Novak, and R. Waterhouse (2009). Mitigation strategy for transmission impairments in millimeter-wave radio-over-fiber networks, *J. of Optical Networking*, 8(2), 201-214
- A. Alphones (2009). Double-spread radio-over-fiber system for next-generation wireless technologies, *J. of Optical Networking*, 8(2), 225-234
- Z. Jia, J. Yu, Y.-T. Hsueh, H.-C. Chien, A. Chowdhury, and G.-K. Chang (2009). Wireless high-definition services over optical fiber networks, *J. of Optical Networking*, 8(2), 235-243.
- Á. A. de G. Vivero, O. Y. Alani, and J. M. Elmirghani (2009). Indoor airport radio-over-fiber network traffic model and performance analysis using load-balancing techniques, *J. of Optical Networking*, 8(3), 272-284.
- S. L. Jansen, I. Morita, N. Takeda, H. Tanaka (2007). 20-Gb/ s OFDM transmission over 4,160-km SSMF enabled by RF-pilot tone phase noise compensation, *OFC 2007*, PDP 15.
- B. Schmidt, A. Lowery, J. Armstrong (2007). Experimental demonstration of 20 Gbit/ s direct-detection optical OFDM and 12 Gbit/ s with a colorless transmitter, *OFC 2007*, PDP 18.
- H. Sasa, T. Niiho, K. Tanaka, K. Utsumi and S. Morikura (2003). Radio-over-fiber transmission performance of OFDM signal for dual-band wireless LAN systems, *MWP 2003*, 139-142.
- A. Kim, Y. Jo and Y. Kim (2004). 60GHz wireless communication systems with radio-over-fiber links for indoor wireless LANs, *IEEE Trans. Consum. Electron.*, 50(2), 517-520.
- J. Yu, M. Huang, Z. Jia, T. Wang, and G. K. Chang (2008). A novel scheme to generate single-sideband millimeter-wave signals by using low-frequency local oscillator signal, *IEEE Photon. Technol. Lett.*, 20(7), 478-480.
- N. J. Gomes, M. Morant, A. Alphones, B. Cabon, J. E. Mitchell, C. Lethien, M. Csörnyei, A. Stöhr, and S. Iezekiel (2009). Radio-over-fiber transport for the support of wireless broadband services, *J. of Optical Networking*, 8(2), 156-178.
- Z. Jia, J. Yu, T. Hsueh, A. Chowdhury, H. Chien, J. A. Buck, G. K. Chang (2008). Multiband Signal Generation and Dispersion-Tolerant Transmission Based on Photonic Frequency Tripling Technology for 60-GHz Radio-Over-Fiber Systems, *IEEE Photon. Technol. Lett.*, 20(17), 1470 – 1472.
- H. Yang, S. C. J. Lee, E. Tangdiongga, F. Breyer, S. Randel, and A. M. J. Koonen (2009). 40-Gb/ s Transmission over 100m Graded-Index Plastic Optical Fiber based on Discrete Multitone Modulation, *in Proc. of OFC 2009*, PDPD8.



Frontiers in Guided Wave Optics and Optoelectronics

Edited by Bishnu Pal

ISBN 978-953-7619-82-4

Hard cover, 674 pages

Publisher InTech

Published online 01, February, 2010

Published in print edition February, 2010

As the editor, I feel extremely happy to present to the readers such a rich collection of chapters authored/co-authored by a large number of experts from around the world covering the broad field of guided wave optics and optoelectronics. Most of the chapters are state-of-the-art on respective topics or areas that are emerging. Several authors narrated technological challenges in a lucid manner, which was possible because of individual expertise of the authors in their own subject specialties. I have no doubt that this book will be useful to graduate students, teachers, researchers, and practicing engineers and technologists and that they would love to have it on their book shelves for ready reference at any time.

How to reference

In order to correctly reference this scholarly work, feel free to copy and paste the following:

Jianjun Yu, Gee-Kung Chang, Zhensheng Jia and Lin Chen (2010). Novel Enabling Technologies for Convergence of Optical and Wireless Access Networks, *Frontiers in Guided Wave Optics and Optoelectronics*, Bishnu Pal (Ed.), ISBN: 978-953-7619-82-4, InTech, Available from:

<http://www.intechopen.com/books/frontiers-in-guided-wave-optics-and-optoelectronics/novel-enabling-technologies-for-convergence-of-optical-and-wireless-access-networks>

INTECH
open science | open minds

InTech Europe

University Campus STeP Ri
Slavka Krautzeka 83/A
51000 Rijeka, Croatia
Phone: +385 (51) 770 447
Fax: +385 (51) 686 166
www.intechopen.com

InTech China

Unit 405, Office Block, Hotel Equatorial Shanghai
No.65, Yan An Road (West), Shanghai, 200040, China
中国上海市延安西路65号上海国际贵都大饭店办公楼405单元
Phone: +86-21-62489820
Fax: +86-21-62489821

© 2010 The Author(s). Licensee IntechOpen. This chapter is distributed under the terms of the [Creative Commons Attribution-NonCommercial-ShareAlike-3.0 License](#), which permits use, distribution and reproduction for non-commercial purposes, provided the original is properly cited and derivative works building on this content are distributed under the same license.

IntechOpen

IntechOpen